

Alois Mbutura
Nairobi, Kenya.

LIST OF SYMBOLS

- c*Speed of light in vacuum or air.*

List of abbreviations

- *LASER*.....*Light Amplification through Stimulated Emission of Radiation*
- *CW*.....*Continuous wave*
- *dB*.....*decibel*
- *TO*.....*Transistor Outline Package*
- *SL*.....*Semiconductor laser*
- *SMI*.....*Self mixing interferometry*
- *FFT*.....*Fast fourier transform.*
- *LEH*.....*Linewidth enhancement factor.*
- *PD*.....*Photodiode*
- *LD*.....*Laser-diode*
- *DAC*.....*Digital-analog converter,*
- *ADC*.....*Analog-digital converter,*
- *SPI*.....*Serial peripheral interface.*
- *OPAMP*.....*Operational amplifier.*
- *TIA*.....*Transimpedance amplifier.*
- *PCB*.....*Printed circuit board.*
- *IC*.....*Integrated circuit.*
- *PSD*.....*Power spectral density.*
- *RMS*.....*Root mean square.*
- *SNR*.....*Signal to noise ratio.*
- *MSB*.....*Most significant bit.*
- *LSB*.....*Least significant bit.*

ABSTRACT

Sensing by LASER phase perturbation otherwise known as LASER interferometry is a powerful measurement tool useful in various applications such as velocity measurement, absolute distance measurement, relative distance change measurement among others. In this report we thus look at LASER interferometry as a tool for vibration measurement as it allows one to perform contactless measurement on a body to sense vibrations to the theoretical accuracy of larger than half a wavelength at the lasing frequency.

This report discusses the design and implementation of a phase detector for LASER phase perturbation demodulation. The implementation chosen is self mixing interferometry as the diode lasers were readily available therefore provided a good starting point to the approach chosen of self mixing interferometry.

The report covers design of a CW diode LASER driver, a transimpedance amplifier on the Photodiode section of the TO-18 laser diode with a -3dB cutoff of 200 kHz, an output high pass filter and the relevant control circuitry that allows the whole system to be tested and controlled with industry standard 32 bit, arduino form factor development boards such as the FREEDOM[®] series from NXP or the DISCOVERY[®] and NUCLEO[®] series from STMicroelectronics among others.

CHAPTER 1: INTRODUCTION

The aim of this project is to develop a phase detector for phase perturbation demodulation in a LASER signal. Phase perturbation is the relative change in phase of a given signal that can be described by its wave characteristics . In this project, a clear distinction between the following is made:

1. A sensing technique based on physical parameters such as phase perturbation of the laser signal as a means to sense and measure a parameter that affects the signal phase in some way.
2. An implementation of the sensing technique to suit the form of the problem at hand such as heterodyne and homodyne implementations of the phase perturbation technique above.

There are many applications and means by which an application of this sensing technique can be used as the measured parameter is carried in the phase change of a LASER signal that thus requires demodulation for the information to be retrieved.

An application of this as per this project is in vibration measurement/vibrometry whereby the vibration of an object/relative movement of an object about a mean position can be sensed. The implementation of this sensing technique is by self mixing interferometry in this project with the advantages:

1. Sensing technique(Phase perturbation)- It is a passive measurement technique thus doesn't require physical contact with the vibrating body.
2. Implementation of the sensing technique(Self mixing interferometry)- Can be performed at low cost and doesn't require accurate alignment of optical sensing equipment.

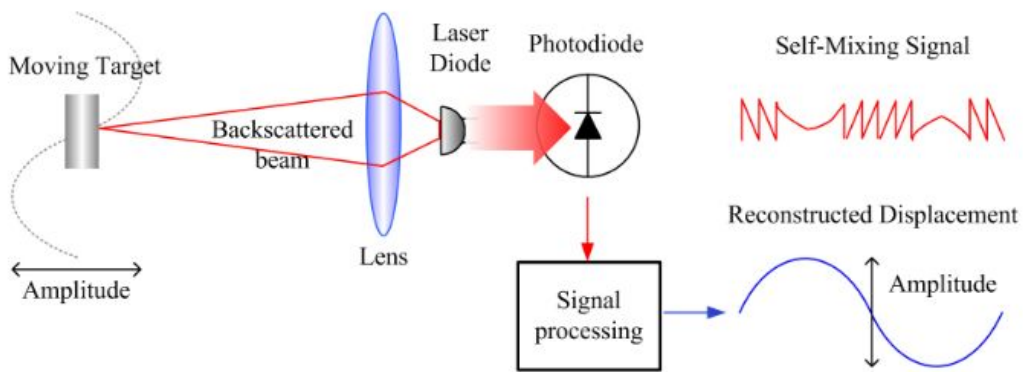
The various sections of this report are outlined as follows:

1. Section 2 discusses theoretical background.
2. Section 3 discusses the optical sensing system design and compromises made.
3. Section 4 discusses the Testing of the phase detector for vibration measurements.
4. Section 5 discusses the results
5. Section 6 discusses the findings in relation to the objectives set prior.
6. Section 7 discusses the possible improvements to the design.

CHAPTER 2: LITERATURE REVIEW

CHAPTER 3: METHODOLOGY

The first course of action was simulating the output of a self mixing technique under certain conditions of the vibrating body such as simple harmonic motion. We thus use the theoretical model developed by Lang and Kobayashi [REF] that is a widely accepted model.



The external light phase without optical feedback at a given point in time for a body under simple harmonic motion is given by:

- $\Phi_0(t)$ is periodically changing light phase with time.
 - ϕ_0 is the light phase at the equilibrium position of a vibrating target given by $\phi_0=2\pi v_0 \tau$.
 τ is the round trip delay of the optical laser signal determined by the external cavity length L. $\tau=2L/c$.
 - f_0 is the frequency of vibration of the external target.

We take the light phase as the phase of the signal at the detector after undergoing a full round trip after reflection off the vibrating target. We thus separate the light phase, from modulated phase as a result of the mixing of the outgoing light and the backscattered light. The modulated phase Φ_E is thus given by:

- Φ_F is the external light phase of an SL with optical feedback modulation. $\phi_f = 2\pi v_F \tau$.

- α is the linewidth enhancement factor of the SL.
 - C is the feedback factor of the SMI setup.

Equation (ii) is a nonlinear equation and we put in the convenient form:

$$\Phi_F(t) - \Phi_0(t) + C \cdot \sin[\Phi_F(t) + \arctan(\alpha)] = 0 \dots \dots \dots \quad (iii)$$

We thus solve this numerically using the `fsolve` function in the scientific python(`scipy`) package, `optimize` subpackage. A solution of Φ_F is thus obtained as a function of time after solving $\Phi_0(t)$ iteratively at each timestep.

If the distance travelled by a wave needs to be described spatially, its wavenumber K is used which describes the 2π radians covered by the wave per unit wavelength in meters. The wavenumber thus can be multiplied by a given distance to obtain the angular shift the wave has undergone in a spatial distance L therefore one can convert between phase and distance by the following relation:

Wavenumber $K = \frac{2\pi}{\lambda}$ (iv)

Angular shift Φ_0 in a distance L travelled by the wave = KL(v)

For a sinusoidal function of the wave, this is a mod(2π) operation.

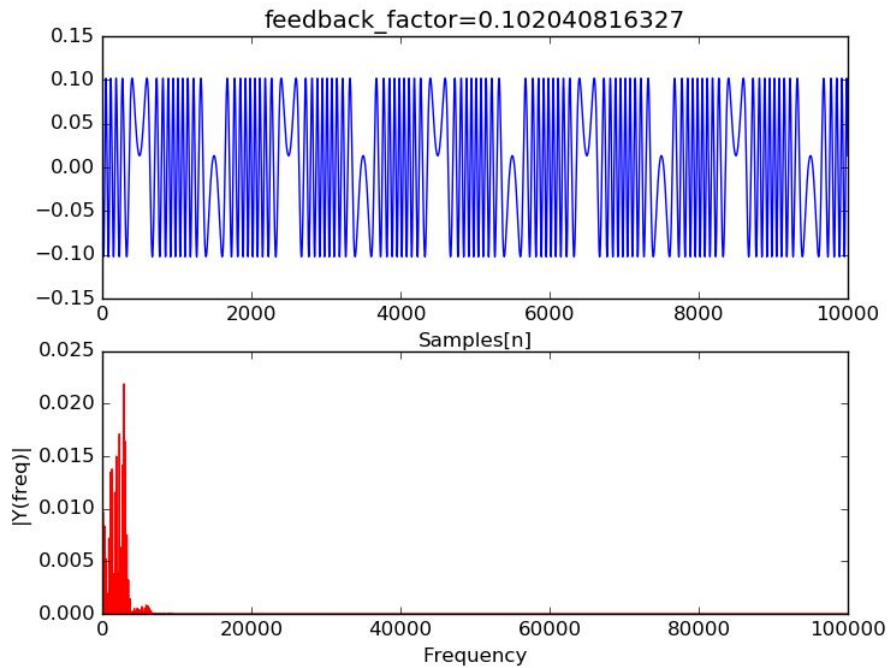
The optical pathlength change as a fraction of the lasing wavelength can be obtained by a modification of the function above:

$\angle L = \beta \cdot \lambda$ (v)

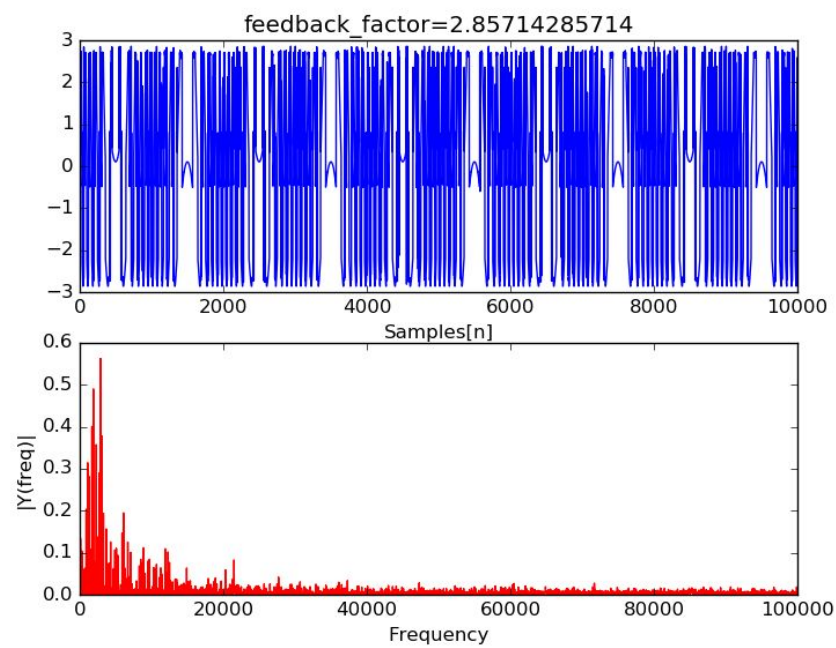
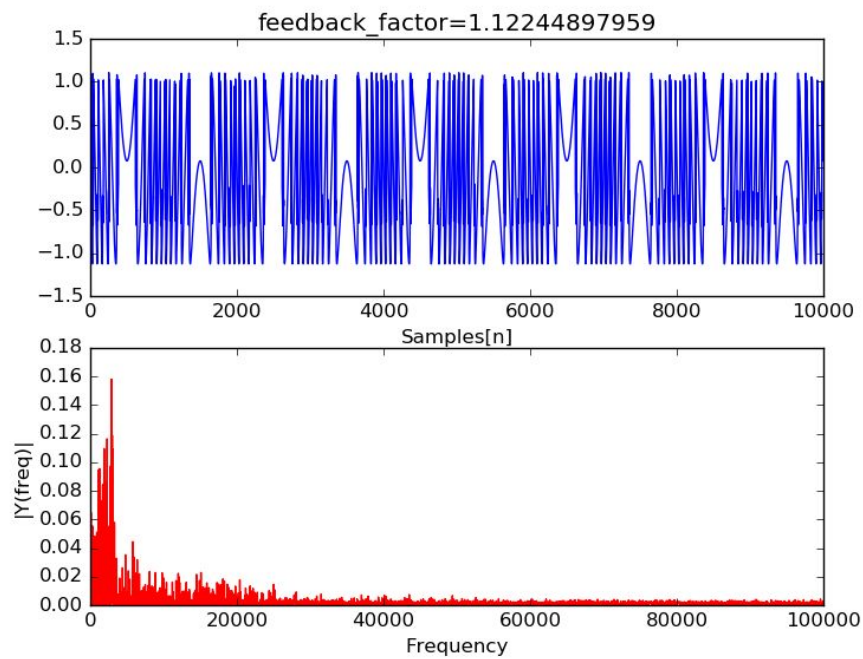
Where $\beta = \frac{\Phi_0}{2\pi}$

We thus take randomly and within good reason $\alpha=3$, $C=0.8$, $\phi_0=0.5\text{m}$, $\Delta\phi=\lambda \text{ rad}$, $f_0=200\text{Hz}$. The individual parameters C , f_0 and α are varied as below and the FFT of the resulting function is taken and plotted.

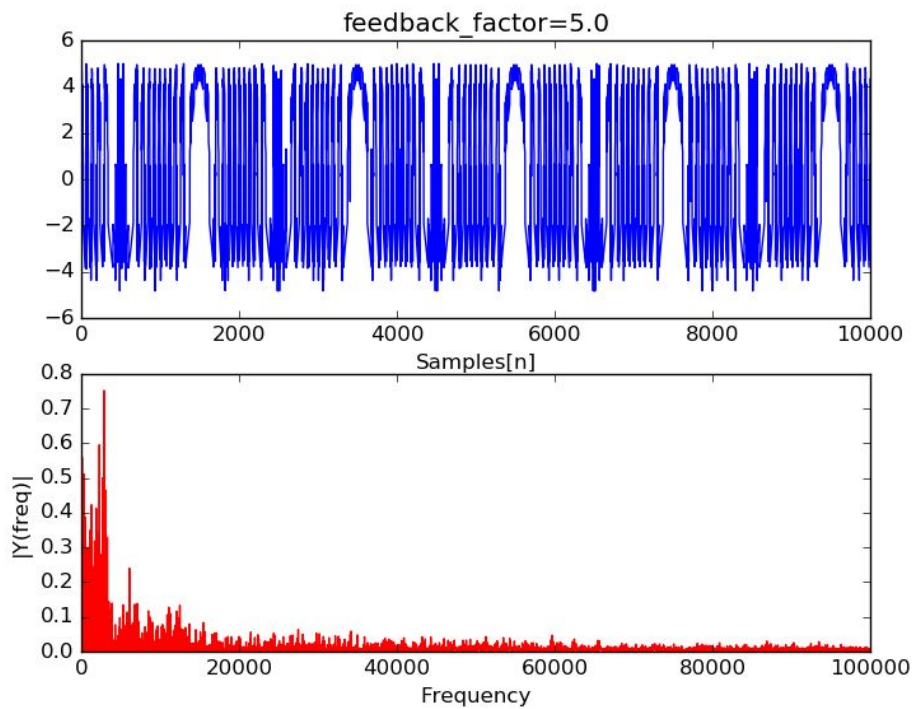
Simulation plots: Feedback factor(C) varied.



Weak feedback($0.1 < C < 1$)-Slight distortion according to literature..



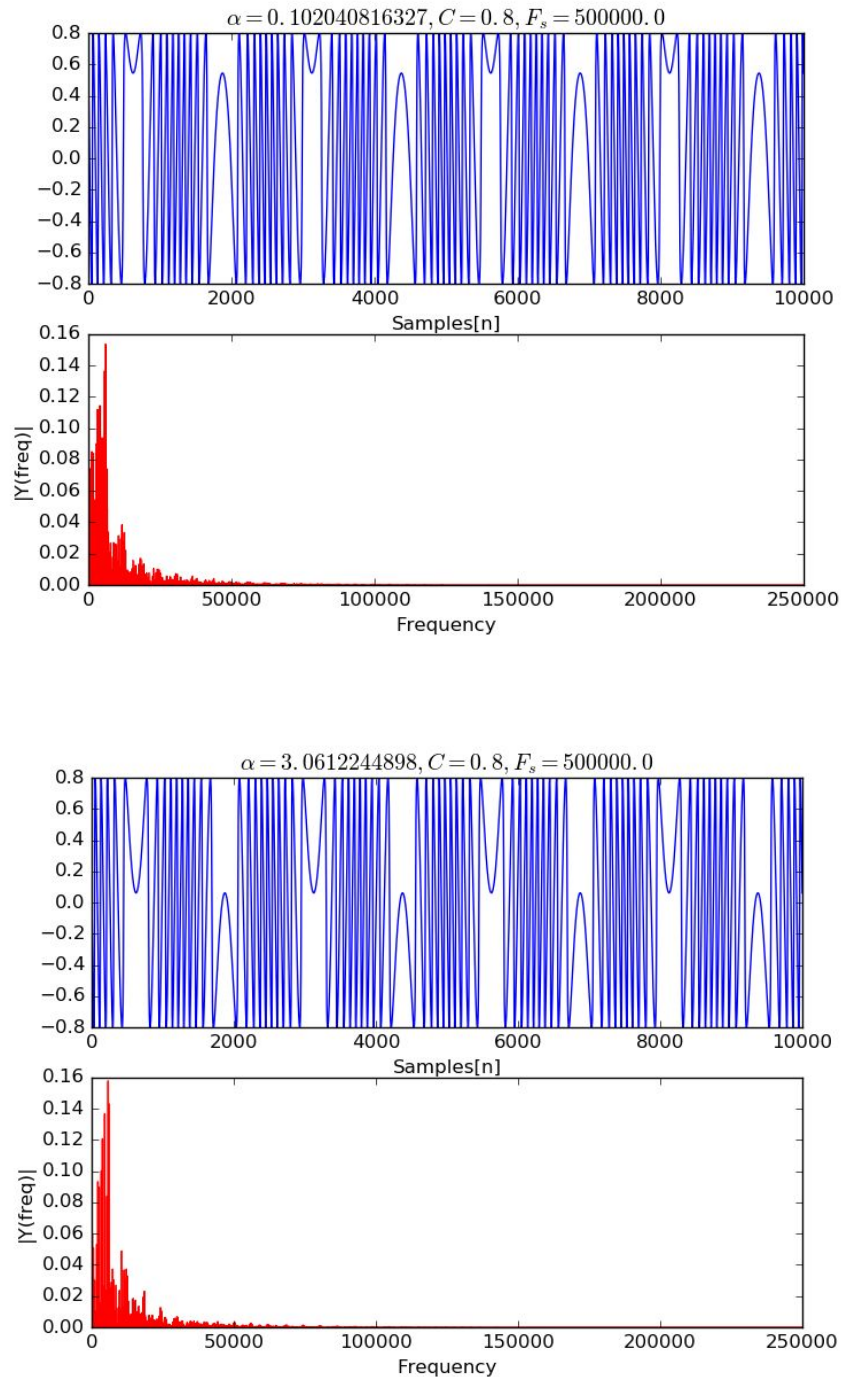
Moderate feedback $1 < C < 4.6$. Sawtooth like and exhibition of hysteresis according to literature..

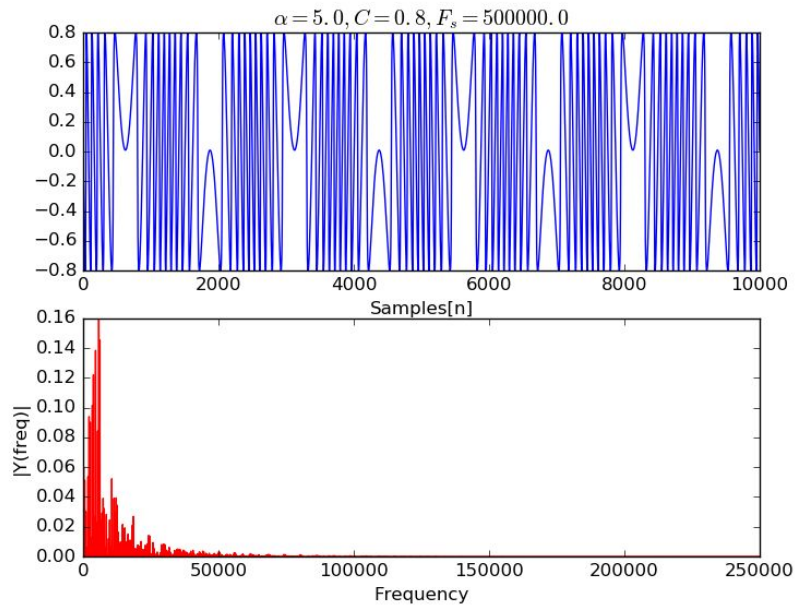


Strong feedback($C > 4.6$). SL goes into mode hopping according to literature.

The parameter C is thus seen to strongly affect interferometric measurements.

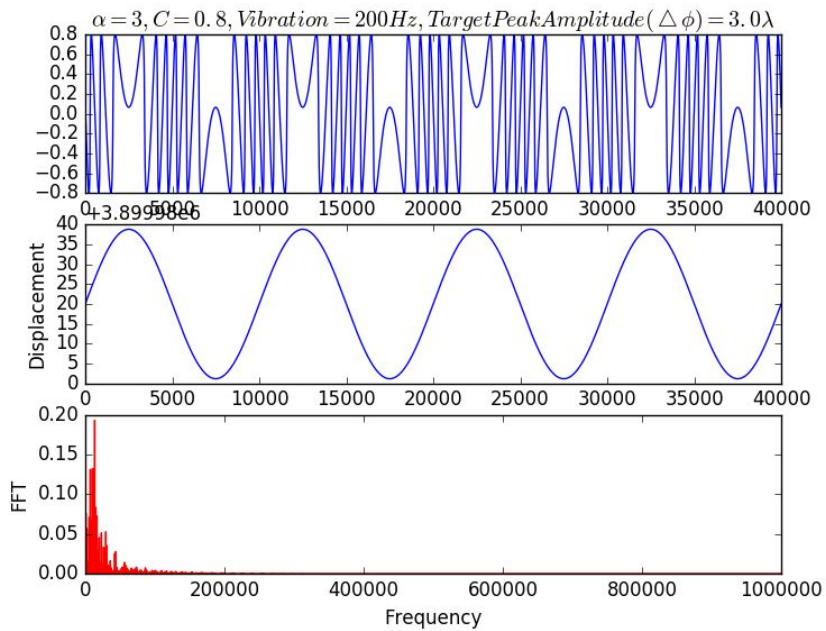
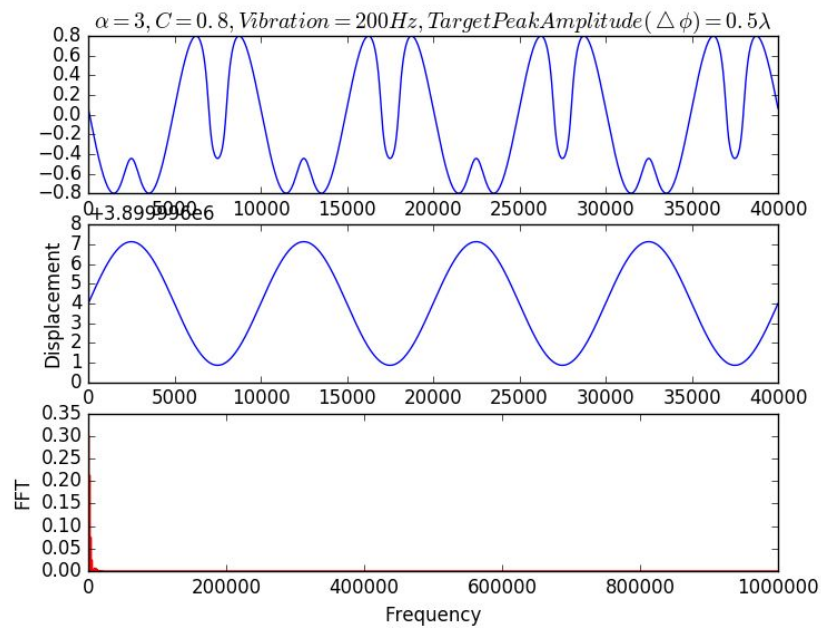
Simulation plots: Linewidth enhancement factor(α) varied.

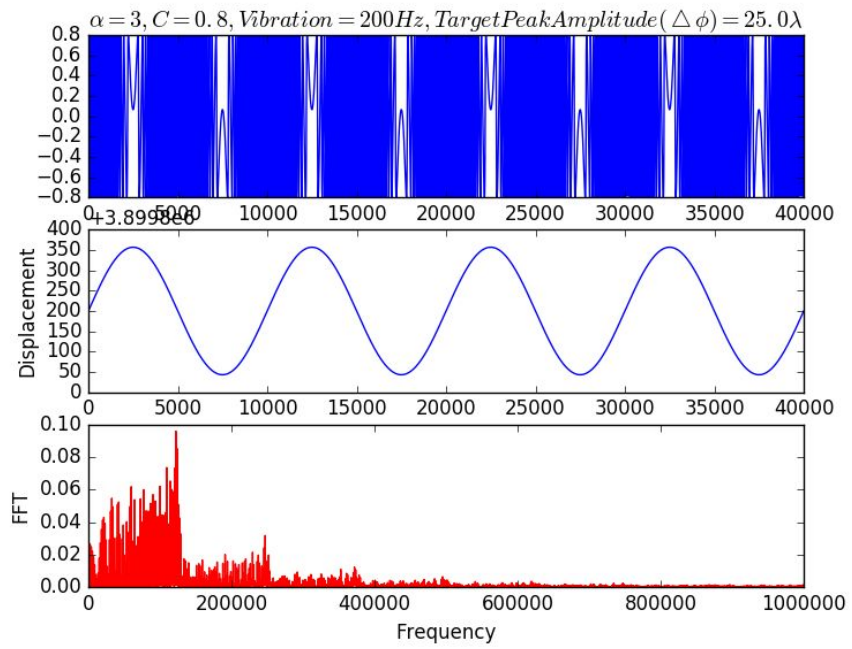
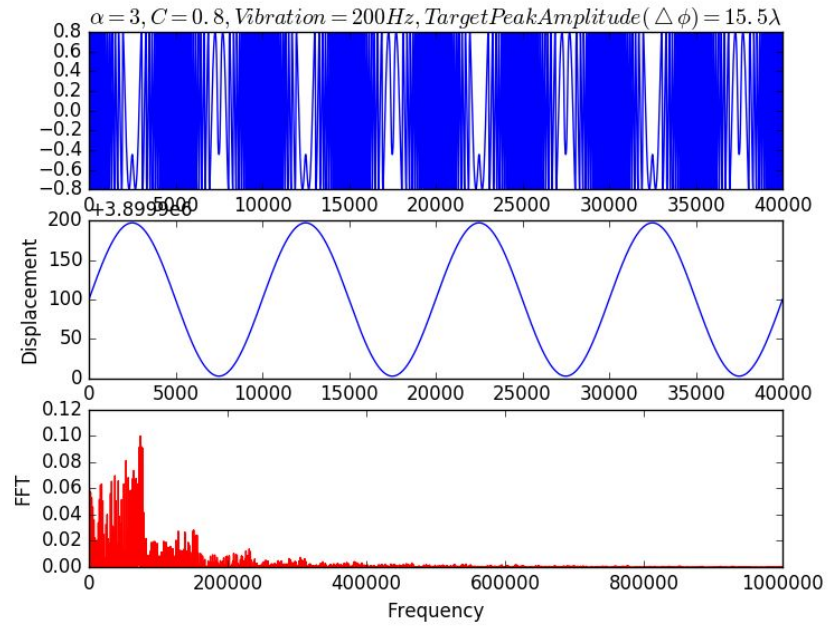




We thus see that the linewidth enhancement factor does not change the frequency content of the signal in terms of varying power spread across the frequency bins of the FFT but the FFT shows a relatively constant power added per frequency bin therefore the effect of the LEH is a relatively constant power spectral density whose power per bin is dependent on the LEH value.

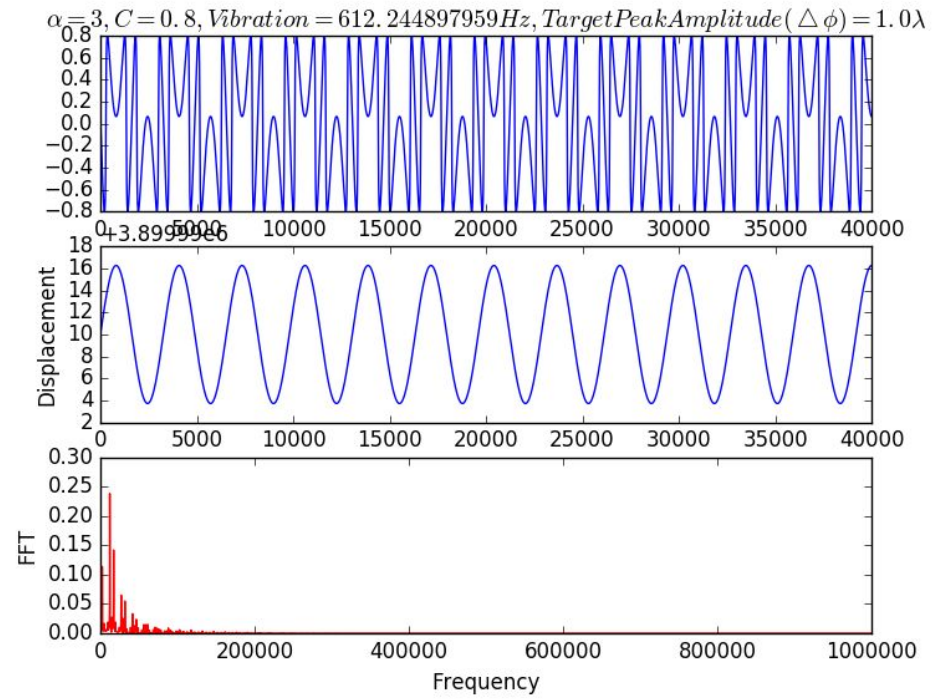
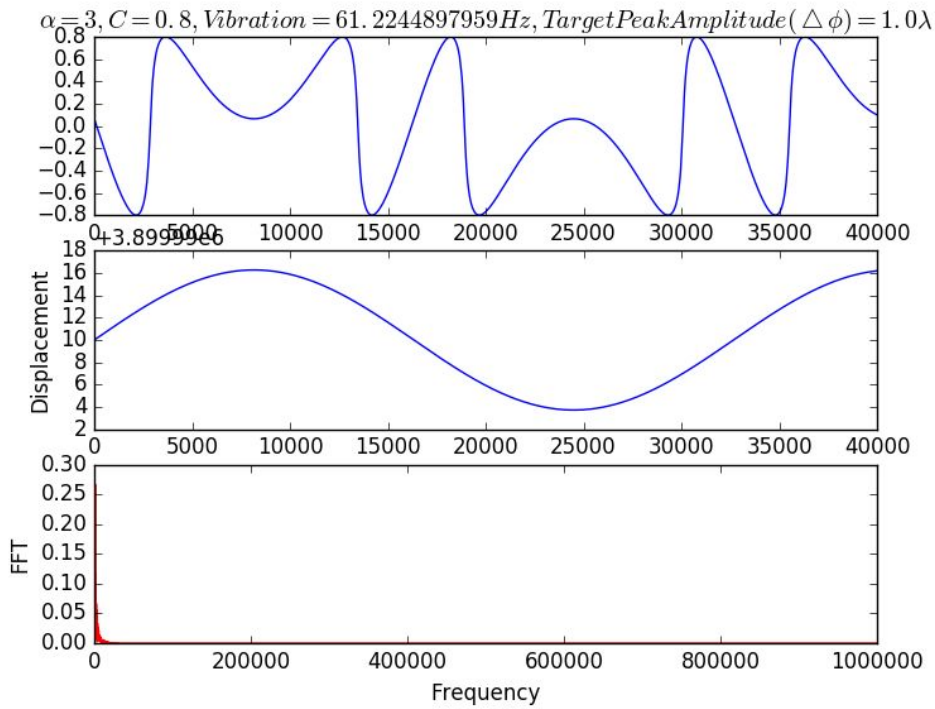
Simulation plots: Target vibrational amplitude($\Delta\phi$) varied.

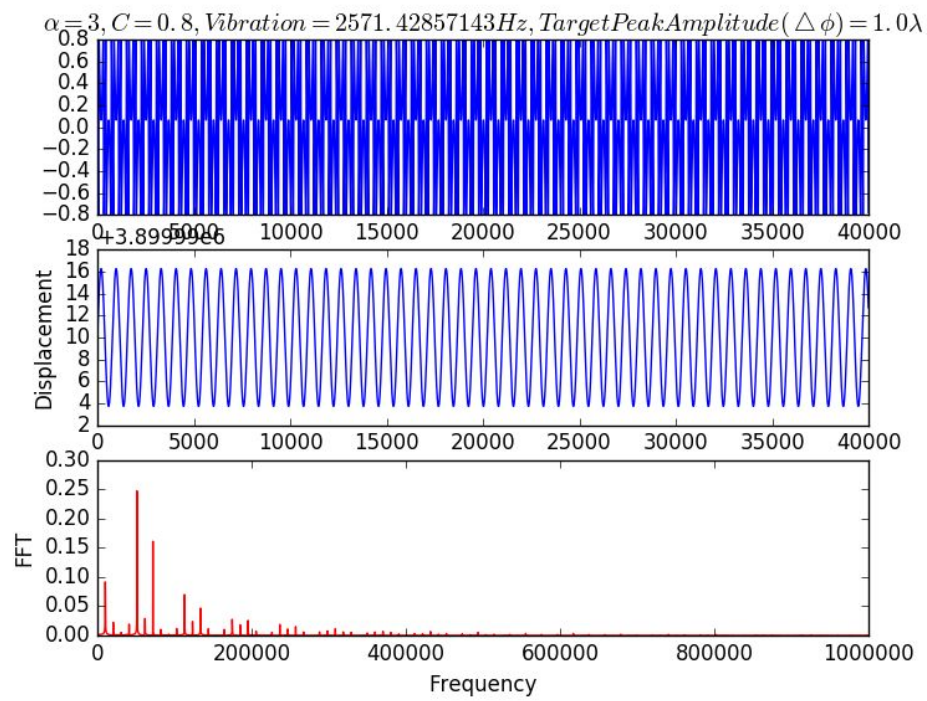
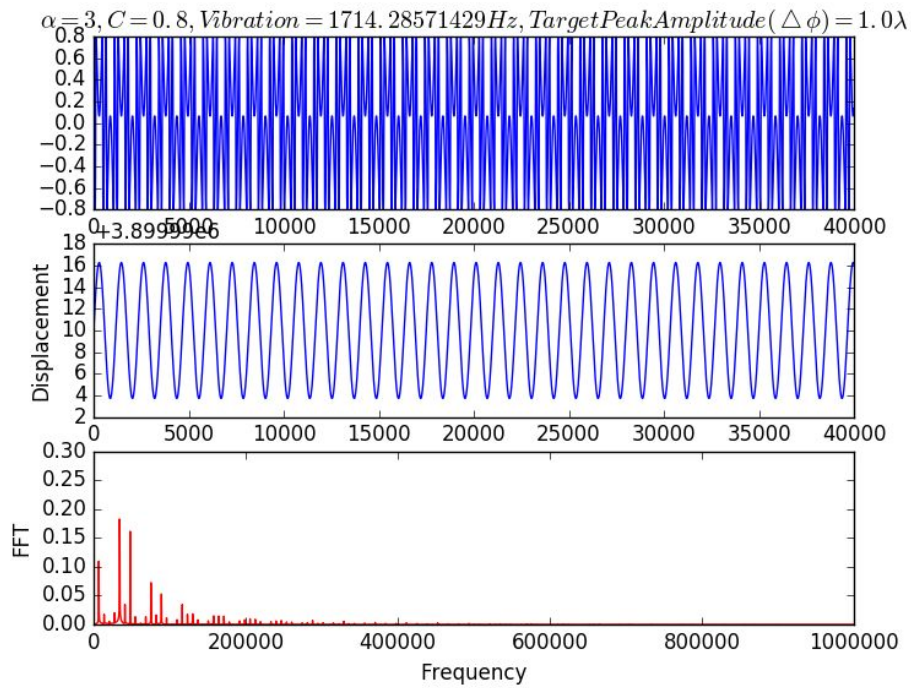


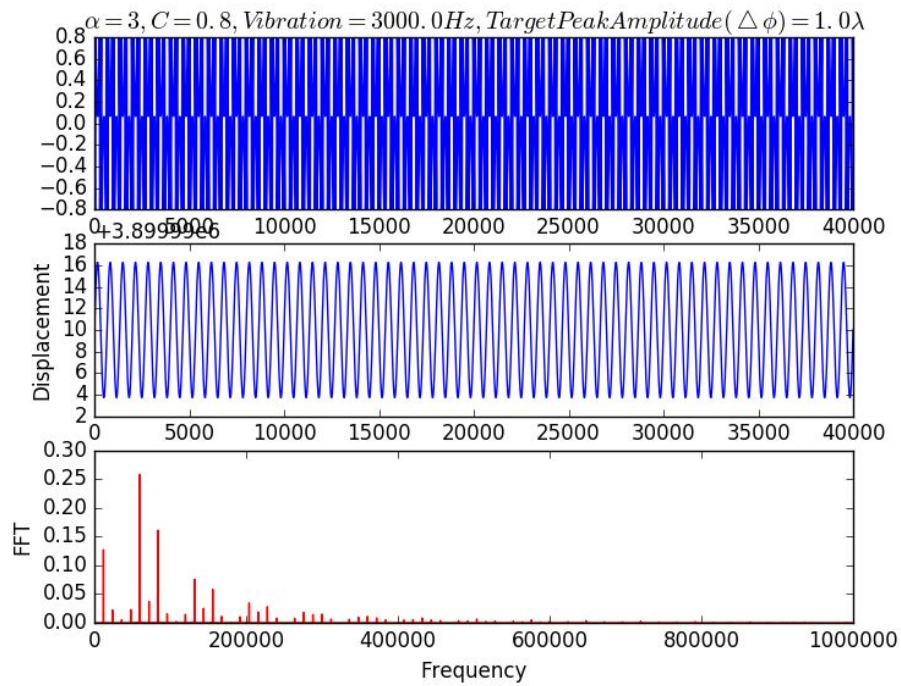


As can be seen, the greater the distance traversed by the vibrating body, the more the interferometric fringes. The displacement amplitude range sought thus sets a constraint on the cutoff frequency of any associated signal processing apparatus.

Simulation plots: Target vibrational frequency(f_0) varied.



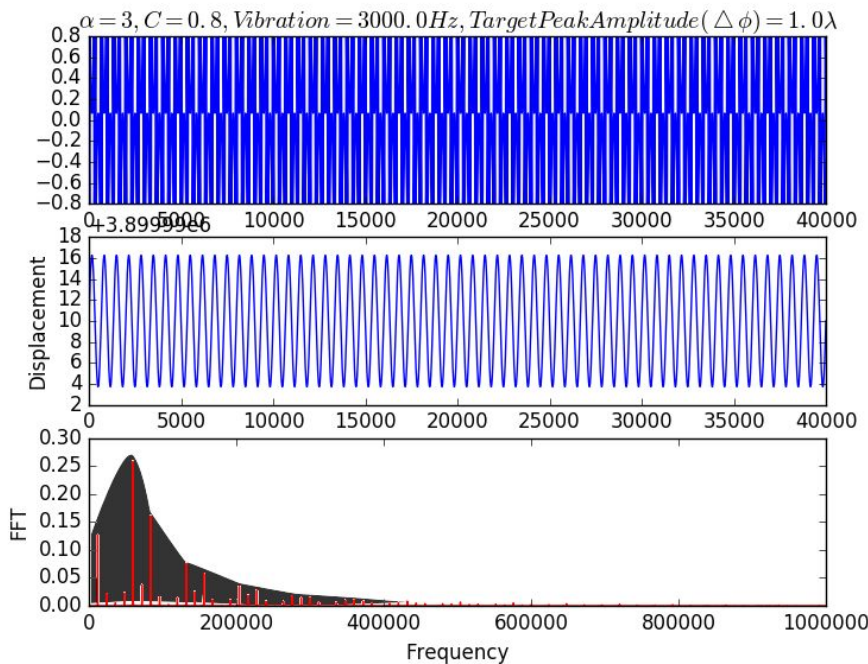


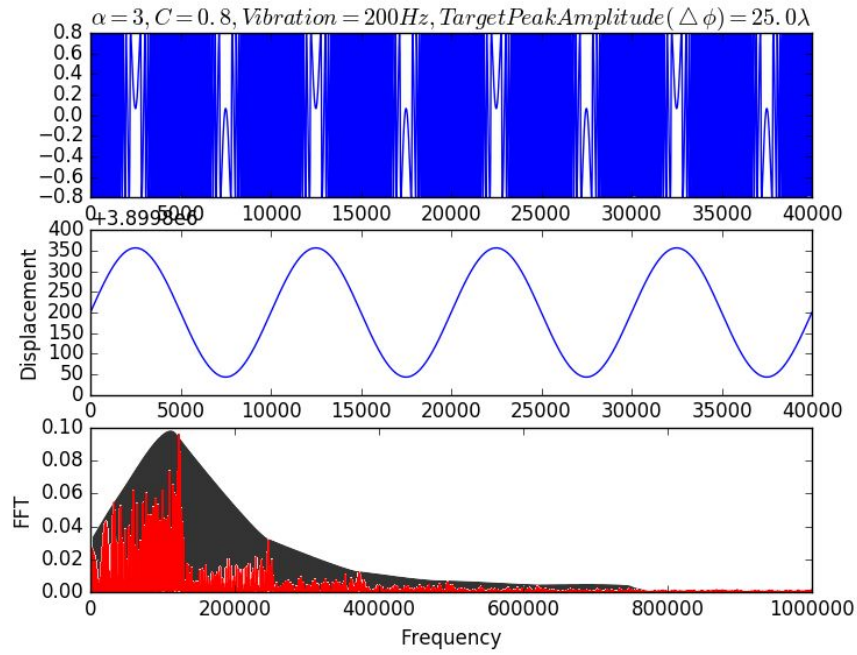


As can be seen, the greater the vibration, the higher the cutoff frequency needed of the signal processing elements due to the greater number of interferometric fringes in the signal per unit time of the resulting interferometric signal although the peak amplitude of the vibrating body and the feedback factor C is held constant at $1.0 \times$ and 0.8 respectively in this simulation trial.

Developing a measure of the “center of mass” of the interferometric spectra to aid in determining the cutoff frequency of signal processing elements.

We thus need to develop a measure of where the mass of the spectra is, for signal processing purposes. The distribution of the frequencies thus needs to be take into account in order to determine the “center of mass” of the resulting spectra of the interferometric signal under our test conditions. As can be seen from the following plots on various variations of f_0 and $\Delta\phi$ _that the distribution of the spectra follows a **poisson distribution** as seen below even for varying C levels.





Since the spectra is not normally distributed, we cannot take the median of the spectra as a measure of the center of distribution of the various frequency magnitudes. We thus calculate a weighted mean of the frequencies present in the interferometric spectra. With their magnitudes as the weights.

$$\text{Normalised spectral centroid} = \frac{\sum_{n=0}^{N-1} f_{bin}(n) Mag(n)}{f_{bin}(n)} \dots \dots \dots (v)$$

To obtain the actual spectral centroid, one needs to multiply the value above by $(Fs/2)$ where Fs is the sampling frequency.

$$\text{Actual spectral centroid} = \text{Normalised spectral centroid} * (Fs/2) \dots \dots \dots (vi)$$

The above formula was put into a python program that used the numerical python toolbox that is useful in vectored array numerical operations. We then simulated a target vibrational frequency spanning the audible frequency range of 0-20 kHz and an target vibrational peak amplitude range of 0-100 λ at the lasing wavelength λ .

The pseudocode is as follows:

-Outer loop 1-Loop through amplitudes 0-100 \times range divided into C=10 steps, init loop counter i:

-Inner loop 1-Loop through frequencies 0-20 kHz divided into C steps, init loop counter j:

-Determine the time domain interferometric signal

-Determine the FFT of the above

-Determine the spectral centroid of the FFT above

-Store value of spectral centroid in array **centroid[j]**

-Store value of current amplitude in array **freq[j]**

-Fit an n order curve on the centroid array values with the frequency array values freq[] as the domain. The resulting curve will have the form

$$\text{FIT_1}(\text{centroid}[j]) = (A_{n-1} \cdot \text{freq}^{n-1} + A_{n-2} \cdot \text{freq}^{n-2} + \dots + A_1 \cdot \text{freq}^1 + A_0)$$

-Obtain the fitting curve coefficients A for the n order curve above and store them in K arrays with size [1xC] where n defines the appropriate order of the fit function with minimal overfitting or underfitting by inspection. In brief, All A_{n-1} values for all C frequencies go into array K_{C-1} , A_{n-2} into K_{C-2} and so on. We shall relate these coefficients to the various amplitude values to obtain an interrelation between amplitude and frequency.

-Outer Loop 2-Loop through the K arrays from K_0 to K_{C-1} :

-Fit an m order curve on the the K_C array values with the amplitude values[] as the domain. The resulting curve will have the form.

$$\text{FIT_2}(K_{c-1}) = (B_{m-1} \cdot \text{Amp}^{m-1} + B_{m-2} \cdot \text{Amp}^{m-2} + \dots + B_1 \cdot \text{Amp} + B_0)$$

where m defines the appropriate order of the fit function with minimal overfitting or underfitting by inspection.

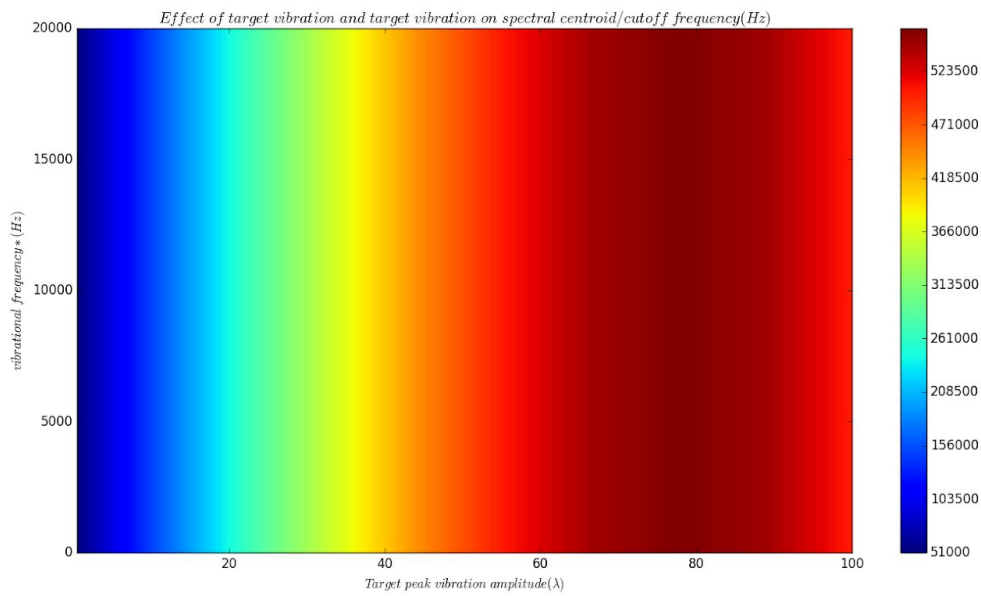
-Obtain the resulting relations between vibrational amplitude and vibrational frequency and their combined linearly approximated effects on the spectral centroid by replacing A_n with the fitted K_C values. $A_{n-1} = \text{FIT_2}(K_{c-1}) = (B_{m-1} \cdot \text{Amp}^{m-1} + B_{m-2} \cdot \text{Amp}^{m-2} + \dots + B_1 \cdot \text{Amp} + B_0)$. n and k have the same size.

-Draw a contour 2D/3D plot over the entire domain using the equation giving the interrelation above:

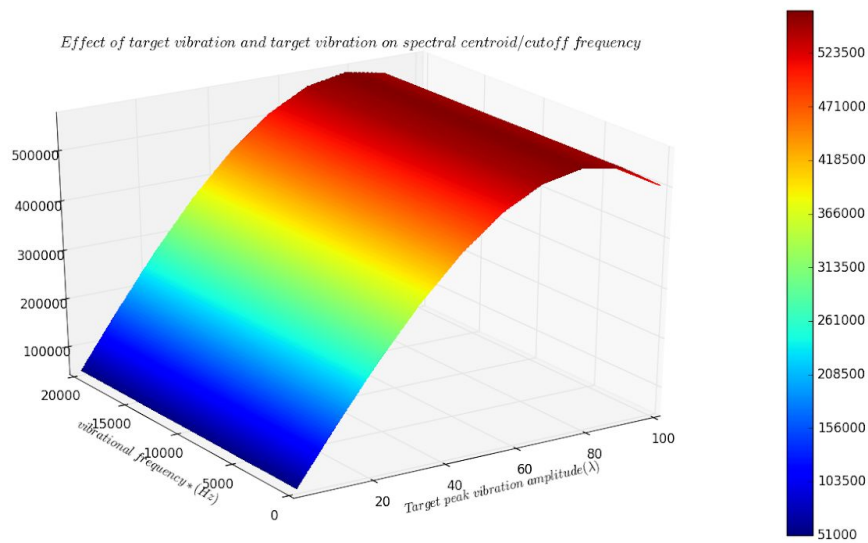
$$\text{FIT_1}(\text{centroid}[j]) = (K_{C-1} \cdot \text{freq}^{n-1} + K_{C-2} \cdot \text{freq}^{n-2} + \dots + K_1 \cdot \text{freq}^1 + K_0), \text{ by expansion:}$$

$$\text{FIT_1}(\text{centroid}[j]) = ((B_{m-1} \cdot \text{Amp}^{m-1} + B_{m-2} \cdot \text{Amp}^{m-2} + \dots + B_1 \cdot \text{Amp} + B_0) \cdot \text{freq}^{n-1} + (B_{m-2} \cdot \text{Amp}^{m-2} + B_{m-3} \cdot \text{Amp}^{m-3} + \dots + B_1 \cdot \text{Amp} + B_0) \cdot \text{freq}^{n-2} + \dots + (B_1 \cdot \text{Amp} + B_0) \cdot \text{freq}^1 + B_0)$$

The above pseudocode gives the below results:



A 3D contour plot gives even more insight:



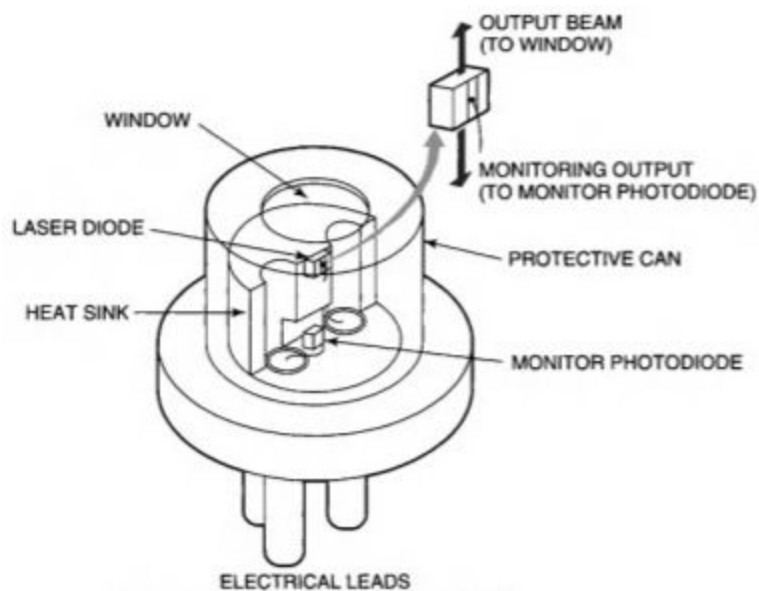
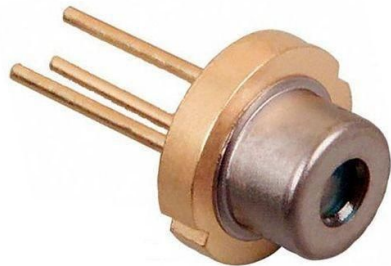
As can be seen which confirms previous simulations that the major factor affecting the cutoff frequency of signal processing elements apart from the value C is the Amplitude range where

one would desire the greatest sensitivity from the interferometer. As can be seen above there is hardly any change in the spectral centroid value with change in vibrational frequency.

Design

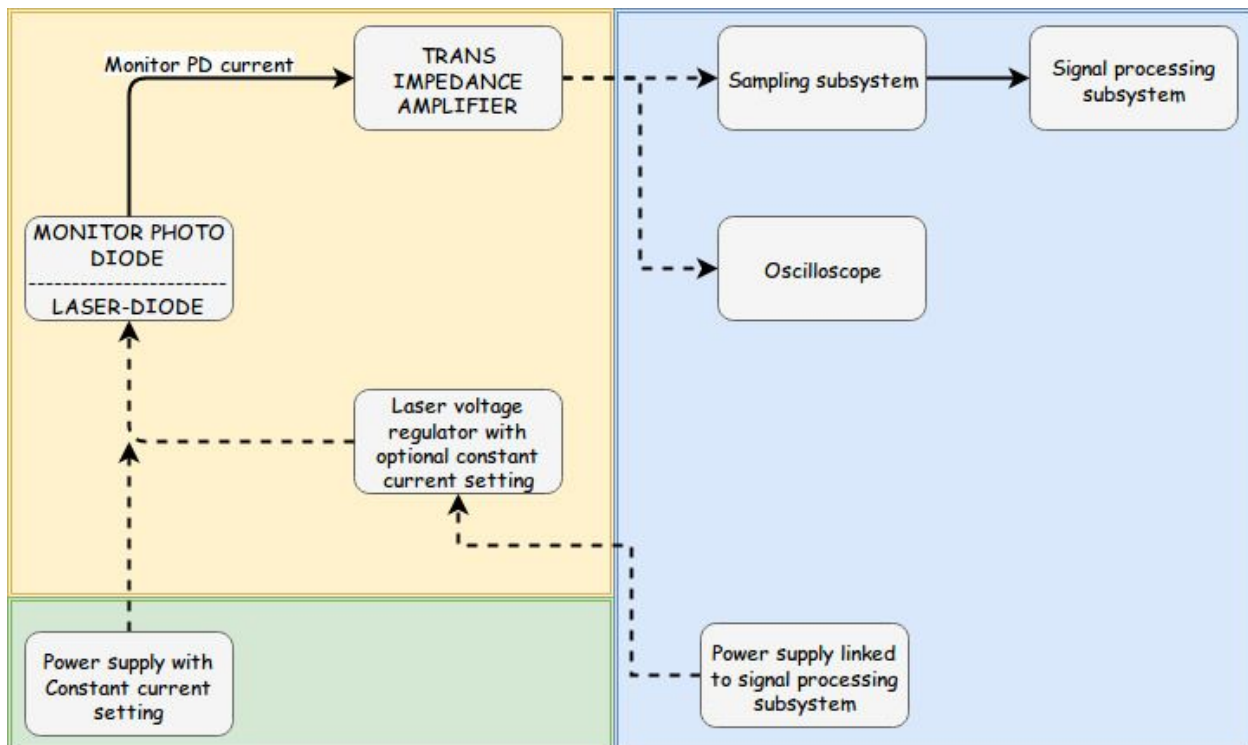
Determination of initial design constraints

- Since there were already present TO-18 SL diodes present at the department, they provided a constraint to the design. These diodes have an photodiode and laser diode within the same package. They are very common in DVD burners and disc readers as the monitor photodiode is used to modulate the power of the SL.



- Another constraint is that the department does not have an optics laboratory thus the design would have to be minimalistic in nature for testing. A foreseen issue is that since an interferometer measures relative vibration about a mean position, if there is disturbance on the sensor, the mean position of the target as observed from the interferometer would change depending on the magnitude of the disturbance. Therefore the design of a true calibrated vibrometer is a mechanical problem as much as it is a sensory problem. Ideally any vibrations/disturbance impact would have to be damped below the actual sensitivity of the device.

Signal processing block diagram

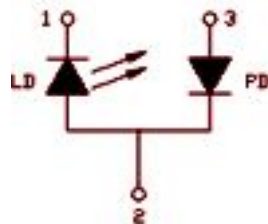


Subsystem determination

- Power supply subsystem.
- LASER diode driver subsystem.
- Photodiode sensing subsystem.
- Highpass filter

LASER diode driver subsystem.

The laser diode has part number ADL-65055TL which is manufactured by LASER components GmbH of Germany. It is an N-type laser diode with a power rating of 5mW. We first determine the laser diode as an N type laser diode. These laser diodes usually have their case tied to their power input terminal. There is a shared pin between the LASER diode and photodiode which means that for the design the LD would have to be forward biased while the PD is reverse biased.



Laser diodes are defined by their applications according to electronic vendor sites such as mouser and thus have different drivers to suit the various applications which fall into two broad categories:

- **CW(Continuous wave laser drivers)**- Are useful in applications where the LASER beam is continuous and unmodulated. Such include sensing applications.
- **Pulsed laser drivers**-Are useful where the laser beam needs Modulation for the application. An example of this application is in telecommunication in Fiber circuits where the laser beam needs to be digitally modulated before transmission through a fibre cable.

Our application is a continuous wave(CW) application thus requires a CW laser driver. The datasheets states the following laser diode parameters:

ADN8810 PARAMETER	VALUE
Light output power	7 mW
Case temperature	-10~+50 deg celsius
Peak wavelength (λ)	655nm
Threshold current	18-25mA
Operating voltage	2.2-2.5v

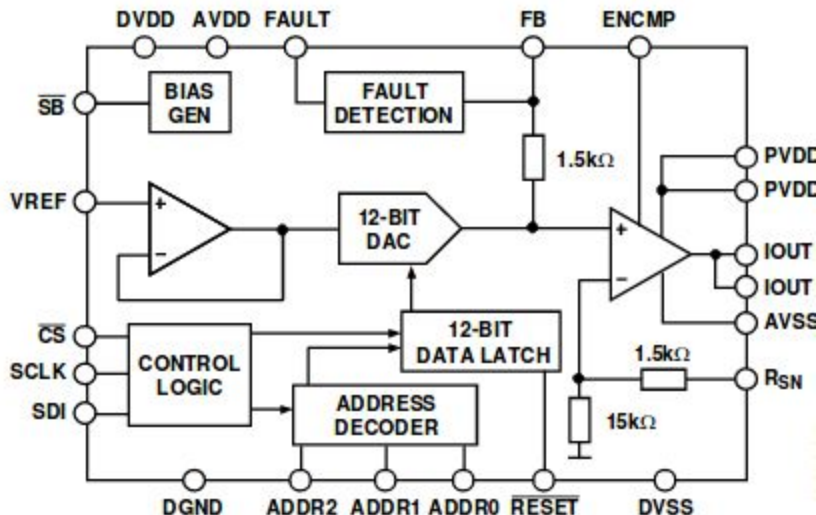
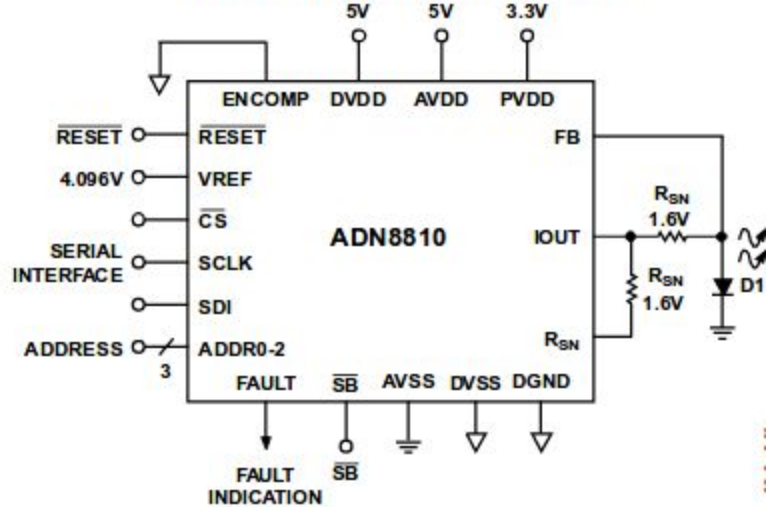
The LASER driver chosen to drive the laser was ADN8810 from Analog devices whose features include:

- High precision 12-bit current source
- Low noise
- Long term stability
- Current output from 0mA to 300mA
- Output fault indication
- Low drift
- Programmable maximum current
- 24-lead 4 mm× 4 mm lead frame chip scale package
- 3-wire serial interface

The intended applications include:

- Tunable laser current source
- Programmable high output current source
- Automatic test equipment

FUNCTIONAL BLOCK DIAGRAM



This allows us to control the driver output current digitally, and note the point in the output current where the laser just begins to lase. Therefore we can use the laser driver as a makeshift optical attenuator to adjust the power. The ADN8810 actually consists of a DAC that converts a 12 bit digital codeword into an analog equivalent in current. For precise control, the ADN8810 requires a separate, precision 4.096v voltage source in order to scale it across the 12 bits giving the DAC a precision reference voltage of 0.001v ideally. As a suggestion, the datasheet gave the analog devices part ADR 292 as a possible candidate.

PIN CONFIGURATION AND FUNCTION DESCRIPTIONS

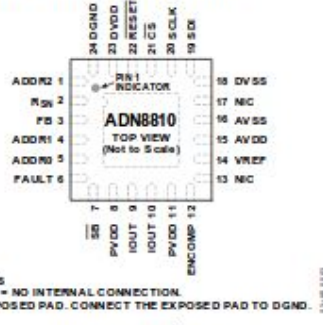
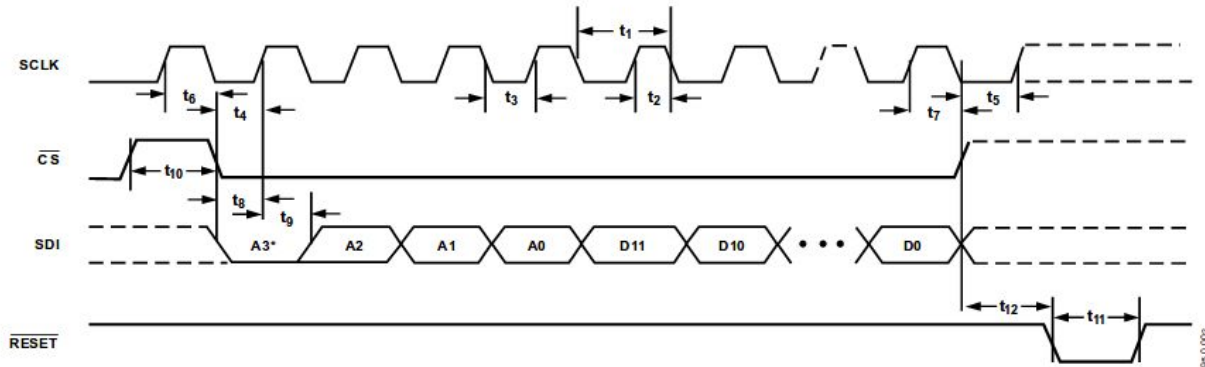


Figure 3. Pin Configuration

Table 4. Pin Function Descriptions

Pin No.	Mnemonic	Type	Description
1	ADDR2	Digital Input	Chip Address, Bit 2.
2	RSN	Analog Input	Sense Resistor RS2 Feedback.
3	FB	Analog Input	Sense Resistor RSI Feedback.
4	ADDR1	Digital Input	Chip Address, Bit 1.
5	ADDR0	Digital Input	Chip Address, Bit 0.
6	FAULT	Digital Output	Load Open/Short Indication.
7	SB	Digital Input	Active Deactivates Output Stage (High Output Impedance State).
8, 11	PVDD	Power	Power Supply for IOUT (3.3 V Recommended).
9, 10	IOUT	Analog Output	Current Output.
12	ENCOMP	Digital Input	Connect to AVSS.
13, 17	NIC	Not applicable	No Internal Connection.
14	VREF	Analog Input	Input for High Accuracy External Reference Voltage (ADR292ER).
15	AVDD	Power	Power Supply for DAC.
16	AVSS	Ground	Connect to Analog Ground or Most Negative Potential in Dual-Supply Applications.
18	DVSS	Ground	Connect to Digital Ground or Most Negative Potential in Dual-Supply Applications.
19	SDI	Digital Input	Serial Data Input.
20	SCLK	Digital Input	Serial Clock Input.
21	CS	Digital Input	Chip Select; Active Low.
22	RESET	Digital Input	Asynchronous Reset to Return DAC Output to Code Zero; Active Low.
23	DVDD	Power	Power Supply for Digital Interface.
24	DGND	Ground	Digital Ground.
0	EPAD	Heat Sink	Exposed Pad. Connect the exposed pad to DGND.

The driver also allows 8 laser drivers to be controlled in parallel on a single communications bus known as the serial peripheral interface(SPI). The timing diagram of the communications protocol is as follows:



*ADDRESS BIT A3 MUST BE LOGIC LOW

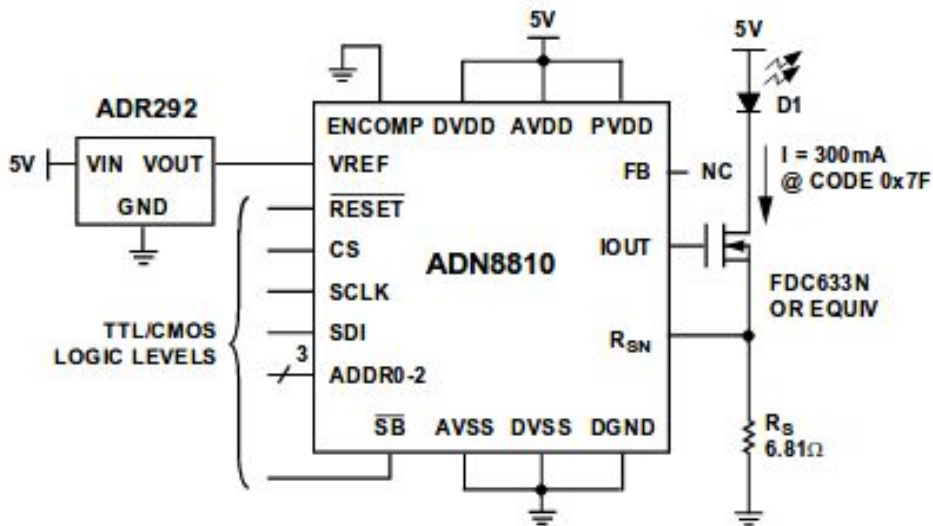
Figx: SPI bus communication protocol

SDI Input	Address Byte				Data Byte											
	A3	A2	A1	A0	D11	D10	D9	D8	D7	D6	D5	D4	D3	D2	D1	D0
Ex. 1	0	1	1	1	0	0	0	0	0	0	0	0	0	0	0	0
Ex. 2	0	0	0	0	1	0	0	0	0	0	0	0	0	0	0	0
Ex. 3	0	1	0	0	1	1	1	1	1	1	1	1	1	1	1	1

Figx: SPI bus packet format

It is worth noting that on the SPI bus, the protocol above caters for a packet width of 2 bytes of which only 15 bits are important[0-14]. 12 bits[0-11] are taken as the code to control the current while 3 bits[12-14] are taken as address bits that allow an address space of 8 laser drivers labelled 0-7. The value of these 3 bits is compared with the voltage setting of the pins ADDR0-3 that aids the driver in determining if a packet is addressed to it. This means that the address of each driver is reconfigurable but this feature is not useful in our application as we have a single laser driver per application.

Within the application section of the datasheet, the following application is given which fits into our problem at hand.



Figx: ADN8810 setup to drive a common-anode to VDD/ N-type LD

We thus need to obtain a mosfet with a low Vgs(threshold) to control the LD.



Figx: SOT-6 package of the FDC637BNZ

The part FDC633N is unfortunately obsolete so as an alternative we choose the part FDC637BNZ above from Fairchild/ON semiconductor as the N-mosfet with the following parameters:

FDC637BNZ PARAMETER	VALUE
Drain to Source Voltage (Vdss)	20v
Current - Continuous Drain (Id) @ 25°C	6.2A
Drive Voltage (Max Rds On, Min Rds On)	2.5V, 4.5V
Vgs(th) (Max) @ Id	1.5V @ 250µA

The mosfet thus can be driven out by a minimum voltage of 1.5v so that the channel starts conduction. Anything below this and the mosfet goes into cutoff. The voltage at the Iout pin of the ADN8810 is given by the following formula:

From the LASER datasheet, the Vfd is given as 2.2v typical to 2.5v max. This gives the range of voltage for I out as:

Therefore the Mosfet will go into conduction with the above parameters.

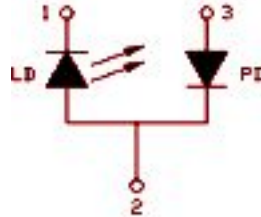
From the datasheet, The voltage at Iout cannot exceed 1 V below PVDD, in this case 4 V when PVDD=5v and 2.3v when PVDD=3.3v. The mosfet thus still goes into conduction.

Resistor R_s sets up the output current by the equation:

$$I = 4.096 \times 1.1 \left(\frac{1}{R_s} + \frac{1}{16.5k} \right) \times \frac{Code}{4096} \quad(vii)$$

The current feedback resistor R_s is the main determinant of the output current. We then choose R_s with value 66.5Ω with a tolerance value of 0.1%. The trace width on the PCB between this resistor and any other component should be wide enough to avoid conduction losses which may introduce a feedback error.

Photodiode sensing subsystem.



Figx: LD-PD N-type configuration

We thus look at the current configuration of the N-type LD-PD package. The photodiode can only be reverse biased therefore the following parameters of the ADL-65055TL are of importance:

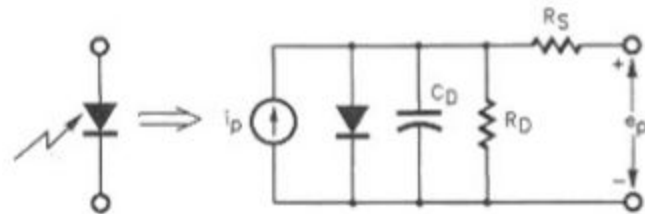
PHOTODIODE PARAMETER	VALUE
Reverse voltage (PD)-Absolute maximum rating	30v
Monitor current	50μA-400μA

In our application, the reverse voltage is 5v therefore does not come close to the absolute maximum rating and therefore gives a safety factor given by the equation below:

$$\text{Safety factor} = \frac{\text{absolute parameter maximum rating}(30\text{v})}{\text{Application parameter value}(5\text{v})}$$

This gives a safety factor of 6 on the photodiode in this application,

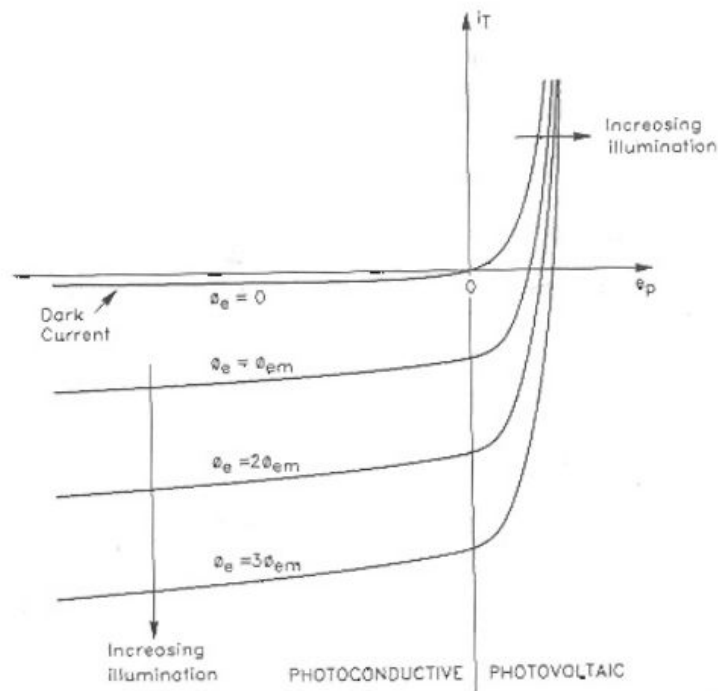
Photodiode model



The photodiode signal is represented by i_p . Resistance R_D represents the diode dark current which is the resistance of its zero biased junction. R_S represents the series resistance of the semiconductor material and it is low enough to be ignored. C_D represents the junction capacitance and has effects on the stability, bandwidth and noise of the photodiode.

There exists two main operating regions of a photodiode:

- **Photoconductive mode**-Is characterised by a photodiode that is reverse biased photodiode. The P-N junction is reverse biased thus the junction capacitance effect is reduced. This thus allows the diode to be used in high speed, high bandwidth systems at the expense of an error introduced due to dark current,
- **Photovoltaic mode**-Is characterised by a photodiode that is forward biased. It is characterised by minimal dark current when biased at 0v. The junction capacitance limits the effective bandwidth of the photodiode.



In our application, the operating mode of the photodiode is the photoconductive mode.

The current from a PD offers far better linearity, offset and bandwidth performance when processing the photodiode signal as opposed to the voltage. The free carriers created in the photodiode by light constitute a current signal. Since the photodiode is a current output device therefore for the purpose of signal processing, there is need to convert it to a voltage. The device that does this conversion is called a **Transimpedance amplifier(TIA)**

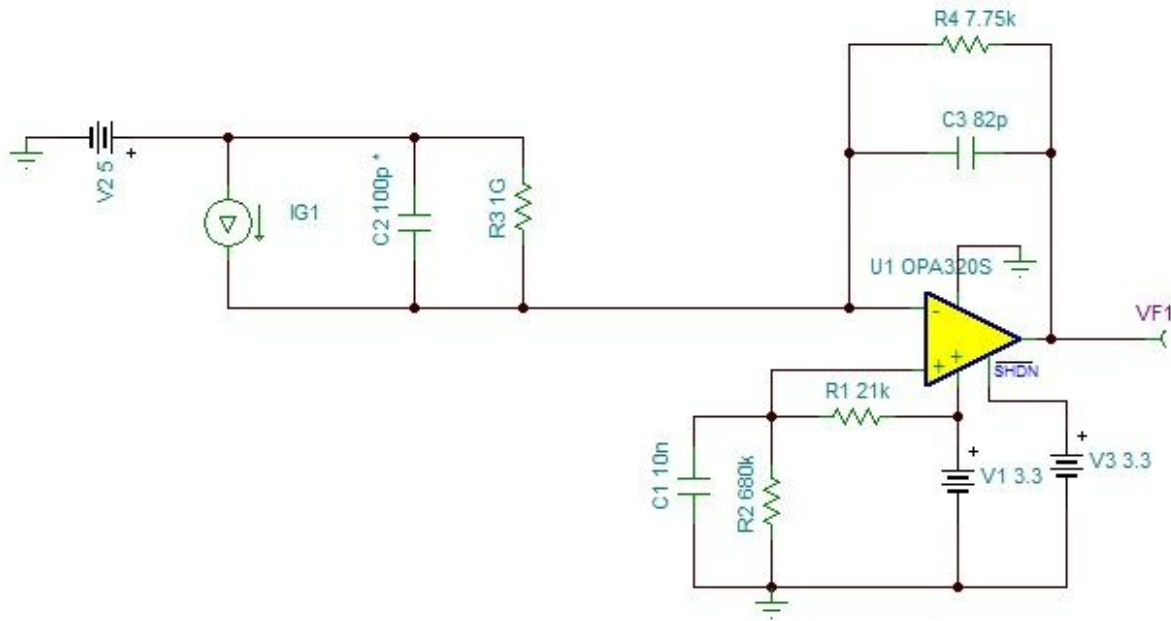
Design requirements

- ***Supply voltage*** 3v3
- ***Supply current*** <10mA
- ***Input current*** 50-400 μ A (From PD-LD datasheet)
- ***Output 100mv-3.2v*** (100 mv less than Vs_{upply}). The TIA output should never settle at Vs_{upply} or GND.

Design goals

- ***Gain(v/A)*** (3.2/0.0004)=8kv/A
- ***Vout for 0uA*** 0.1v
- ***Vout for 400uA*** 3.2V
- ***-3dB bandwidth*** 250 kHz(So that the sampling and signal processing subsystem can sample at ≥ 4 times the -3dB bandwidth)
- ***Phase margin:*** >45 degrees.

The design below though is explained from an analysis point of view though at the time of design it is The following TIA circuit is thus designed in TINA-TI SPICE simulation tool from Texas Instruments:



An important parameter that is important for simulation is the junction capacitance of the PD but this value is not stated in the datasheet which makes us come to two assumptions:

- The PD junction capacitance is a poorly controlled parameter.
- The PD junction capacitance was not viewed as important by the manufacturer for the applications that the diode would be used for as essentially the monitor photodiode is meant to modulate the LD power and primarily not used directly.

The capacitance was thus simulated from 1pF to 1200pF in each simulation, including stability. The photodiode series resistance was neglected for the simulations due to the reasons stated. The shunt resistance was taken as $1\text{G}\Omega$.

Determining DC transfer function

Feedback resistor

We first determine the feedback resistor value. This is used to set the gain of the system by the equation:

$$\frac{V_{out(max)} - V_{out(min)}}{I_{in(max)}} = \frac{3.2V - 0.1V}{0.0004} = 7.75k\Omega \dots\dots\dots(viii)$$

The 7.75k is thus truncated to 7.87k Ω (E96/E192)

V_{out(max)} and V_{out(min)} and determined by the ADC input voltage range. For a typical STM32 microcontroller this is 3.3 volts to 0.1 Volts. We have chosen the output voltage to swing within 100mv of either rail. The common term for OP AMPS that have this characteristic are described as “rail to rail” OP AMPS.

We need the OP AMP to operate in a single supply configuration with the negative rail being a ground connection. Therefore the open-loop transfer function of an OP AMP is given by:

$$V_{out} = A_d(V^+ - V) \dots\dots\dots(ix)$$

For no input on the inverting input, the OP AMP output settles on a the non inverting input which is given by:

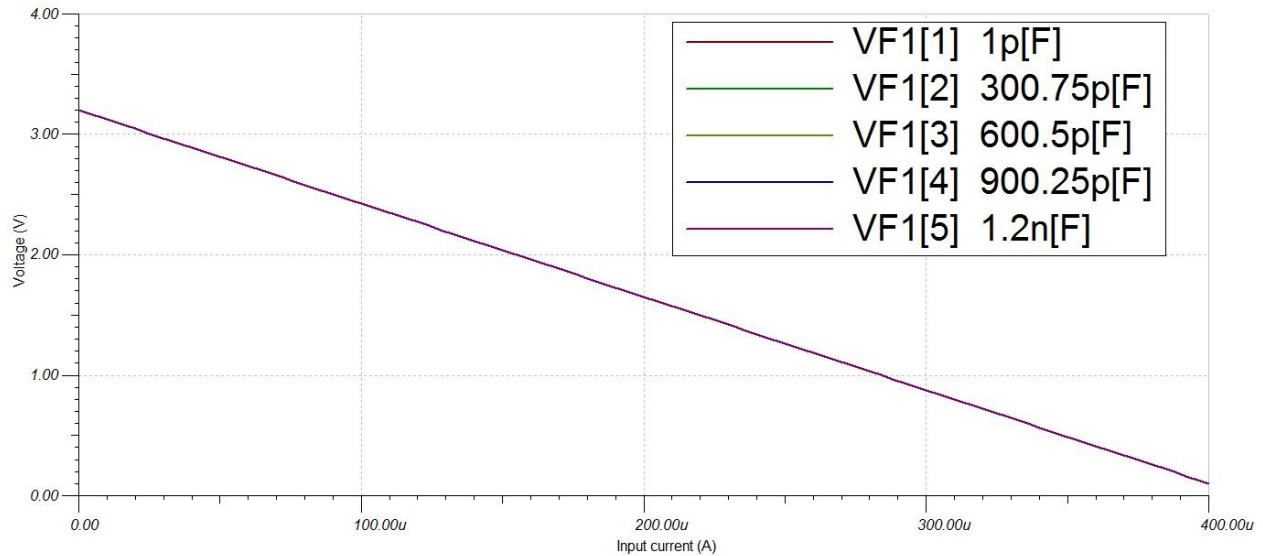
$$V_{out} = A_d(V^+) \dots\dots\dots(x)$$

Since the PD is reverse biased in the photoconductive region, the anode of the Photodiode becomes more negative with respect to the cathode for increasing illumination. With no illumination, the output of the photodiode is only dark current. The V⁺ thus is set at 3.2 volts in order to allow the output rail to swing within 100mv of the positive supply rail.

$$(V^+)3.2v = \frac{R_2}{R_1+R_2} V + supply(3.3v) \dots\dots\dots(xi)$$

R₂=680k(E24) and R₁=21k(E96/E192). Due to their use in setting a bias point, these resistors should have a tolerance of 1% or better.

This gives the following DC transfer function of the TIA:



Determining AC transfer function

Feedback capacitor

The feedback capacitor C is used for the main purpose of :

- Determining system stability and therefore system rise time, settling time and gain peaking.
- Setting the frequency breakpoint/-3dB bandwidth.

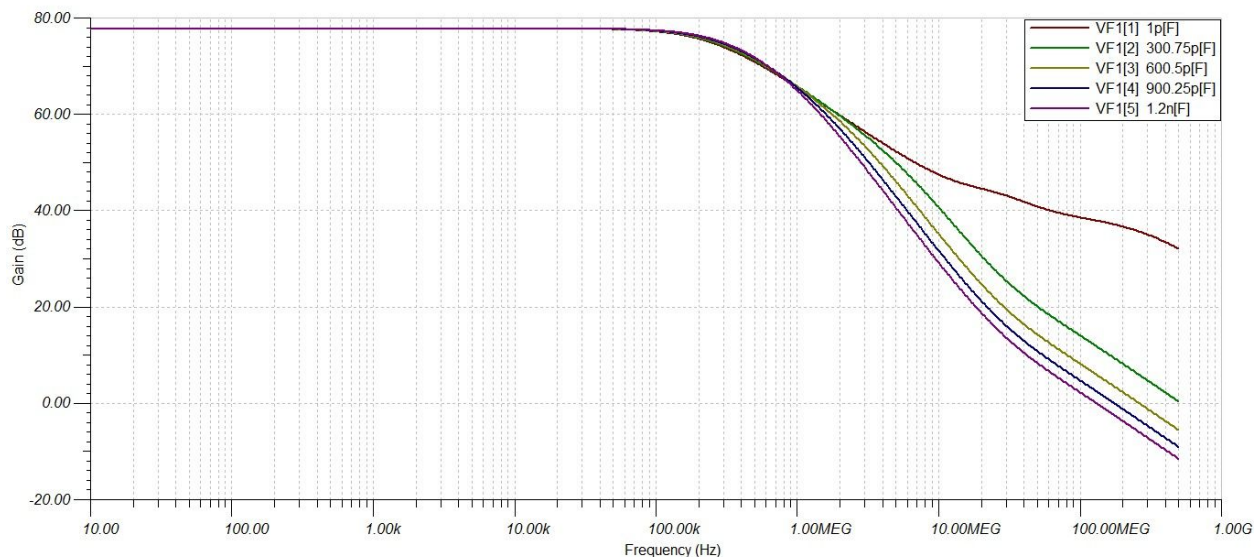
We thus choose our bandwidth as 250kHz. According to our analysis of the theory above, for a feedback parameter C of 0.8, this gives target peak vibration amplitude ($\Delta\phi$) of 30 \times . At the lasing typical wavelength of 655 nm, the maximum measurable is 0.02mm for a feedback factor value of 0.8. The lower limit of detection shall be evaluated in a later section and thus will be bounded by the noise floor of the system.

With increasing feedback coupling into the laser diode cavity, the upper bound of the measurable target peak vibration amplitude will decrease. There is thus a need to actively determine feedback factor while the device is in operation.

$$F_{break} = \frac{1}{2\pi RC} \dots \dots \dots (xi)$$

C is chosen as 82pF(E12/E24) after substituting R=7.75k and F_{break}=200kHz. No truncation is performed on the capacitor value to get it to a valid value.

The above capacitor value gives the following AC transfer characteristic:



All values of junction capacitors have their cutoff frequencies in the 250-320 kHz range. The gain level in the above plot is not normalised at 0 dB therefore -3dB point is
Passband(dB)-3dB= \sim 74.77dB.

The -3dB point per junction capacitance is as follows:

- 251.94 kHz at 1 pF
- 263.46 kHz at 300.75 pF
- 275.5 kHz at 600.5 pF
- 292.43 kHz at 900.25 pF
- 310.39 kHz at 1.2 nF

Determining stability

We need to calculate the opamp gain bandwidth for the circuit to be stable. The capacitance as seen from the inputs consists of various components including:

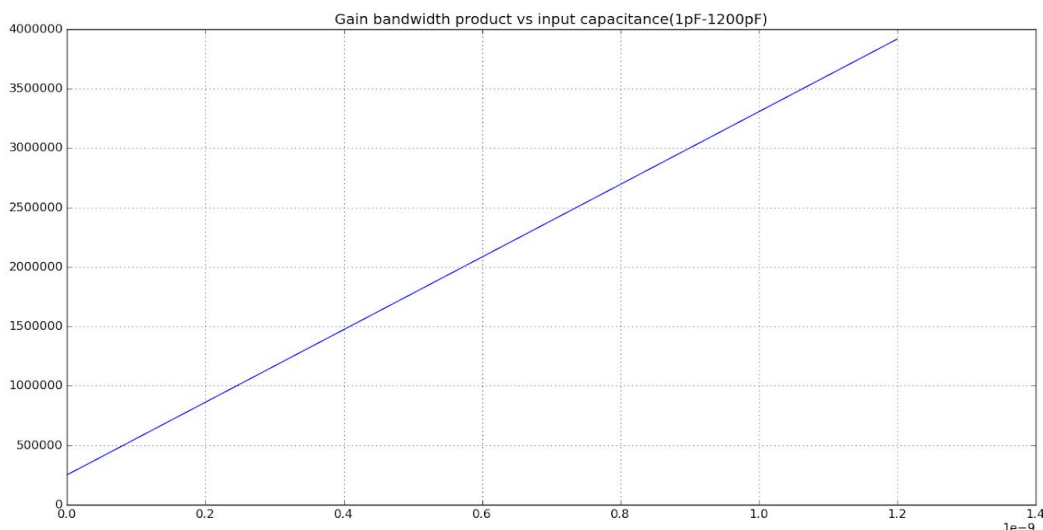
- Photodiode junction capacitance.
- OP AMP differential capacitance.
- OP AMP common mode capacitance.

$$\text{Therefore } C_{in} = C_{junction} + C_{common} + C_{diff}$$

According to [REF] this capacitance can help calculate the minimum gain bandwidth product by the equation:

$$F_{GBW} > \frac{C_i + C_1}{2\pi R C} \dots \dots \dots \text{(xiii)}$$

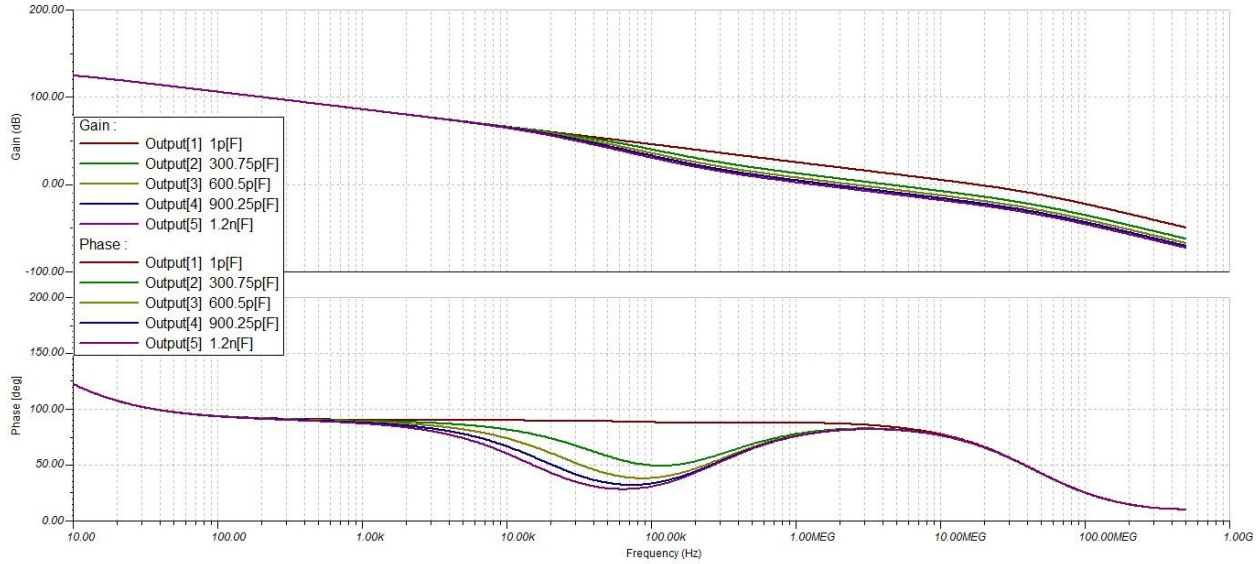
The minimum gain bandwidth product was thus calculated for varying values of input capacitance(junction capacitance) using a python program that gave the Minimum Gain bandwidth needed as 4MHz @ 1200pF.



The OPA320 was chosen from all the above criteria as it has a Gain bandwidth product of 20 MHz.

A PSPICE method that is used to determine stability according to [REF] involves inserting a large inductor and capacitor in the amplifier's feedback loop that opens the loop for AC signal and keeps it closed for DC.

This gives the following stability plots:



The phase margin at the maximum and minimum junction capacitances were:

1pF:Phase margin: 69.18 degree at frequency (Hz): 17.21MEG

1200pF: Phase margin: 78.13 degree at frequency (Hz): 1.30MEG

The various values of capacitances in between follows a linear pattern in terms of the frequency and phase margin.

We thus need to determine the full power bandwidth of the circuit with the constraint that:

$$\text{full-power bandwidth} > -3\text{dB bandwidth} \dots \dots \dots \text{(xiv)}$$

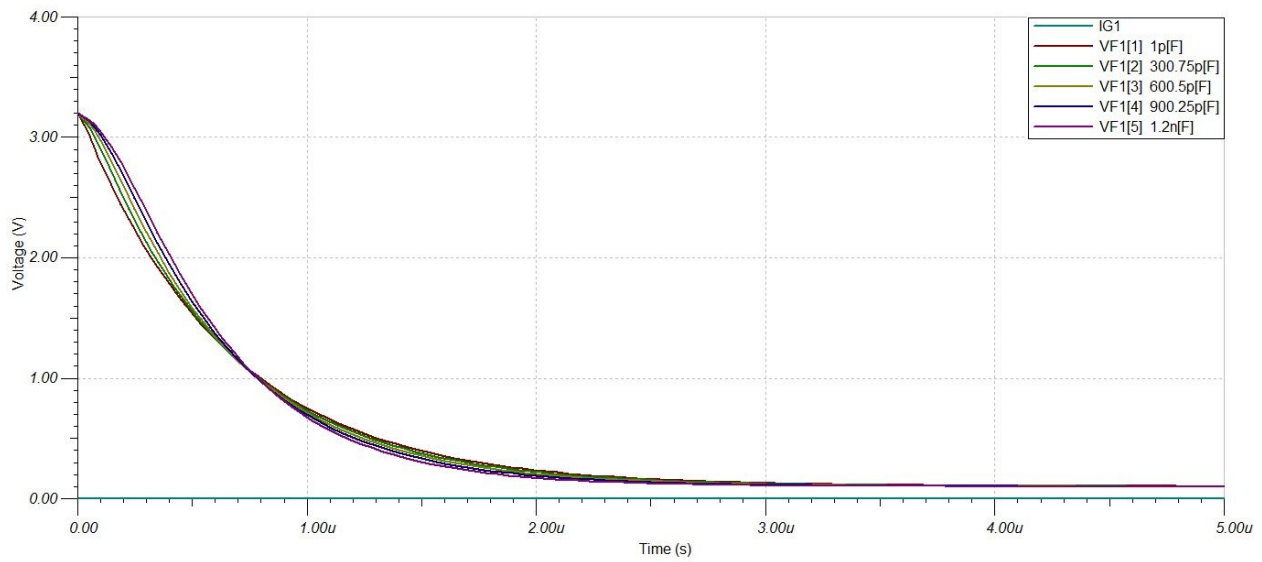
The full power bandwidth is affected by the slew rate of the OP AMP and is given by:

$$\text{full-power bandwidth} = \frac{SR}{2\pi A} \dots \dots \dots \text{(xv)}$$

$$SR = 10V/\mu s, A = 3.2/2 = 1.6$$

$$\text{full-power bandwidth} = \frac{10 \times 10^6}{2\pi(1.6)} = 994.7 \text{kHz}$$

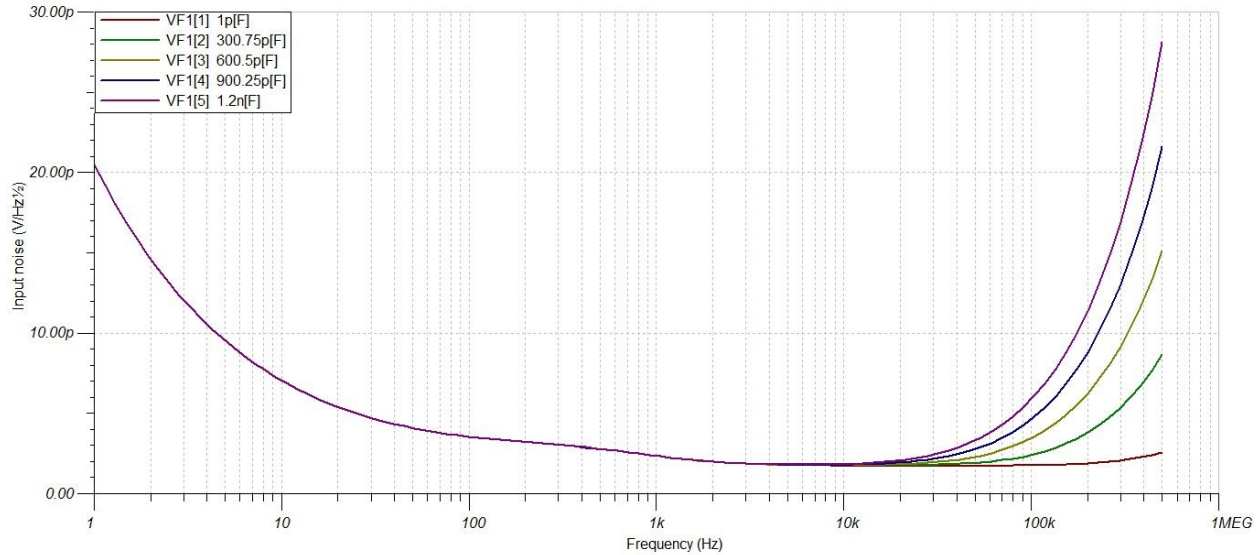
The above give design the following step response for a step input 0-400 uA for the junction capacitance range 1pF to 1.2nF simulated.



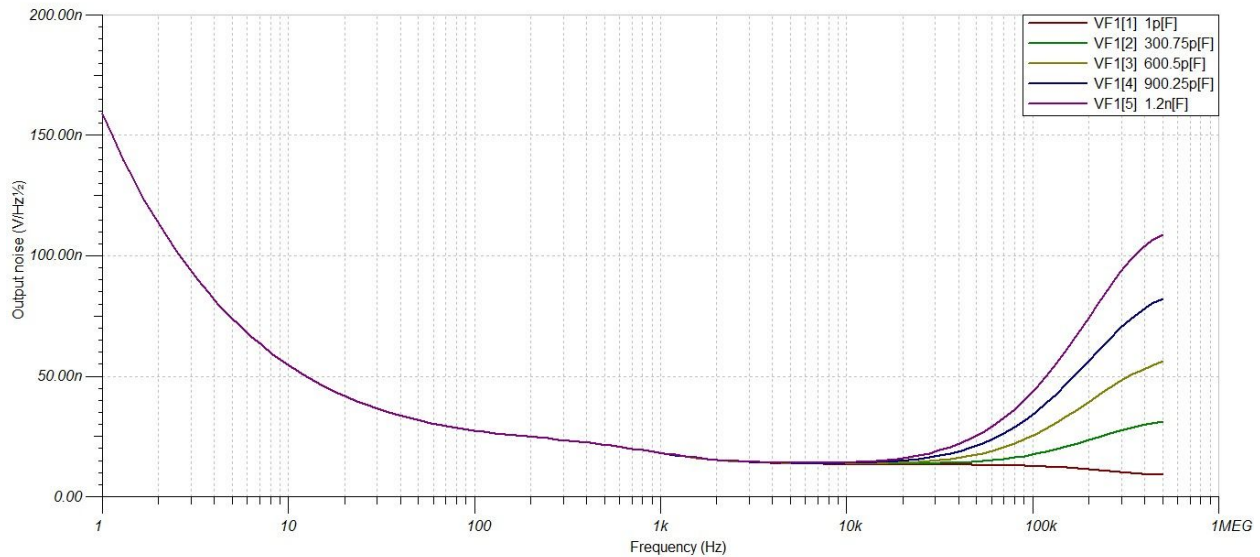
Step response: The system thus is stable over the range with no ringing or overshoot.

Determining the lower sensitivity limit/noise floor

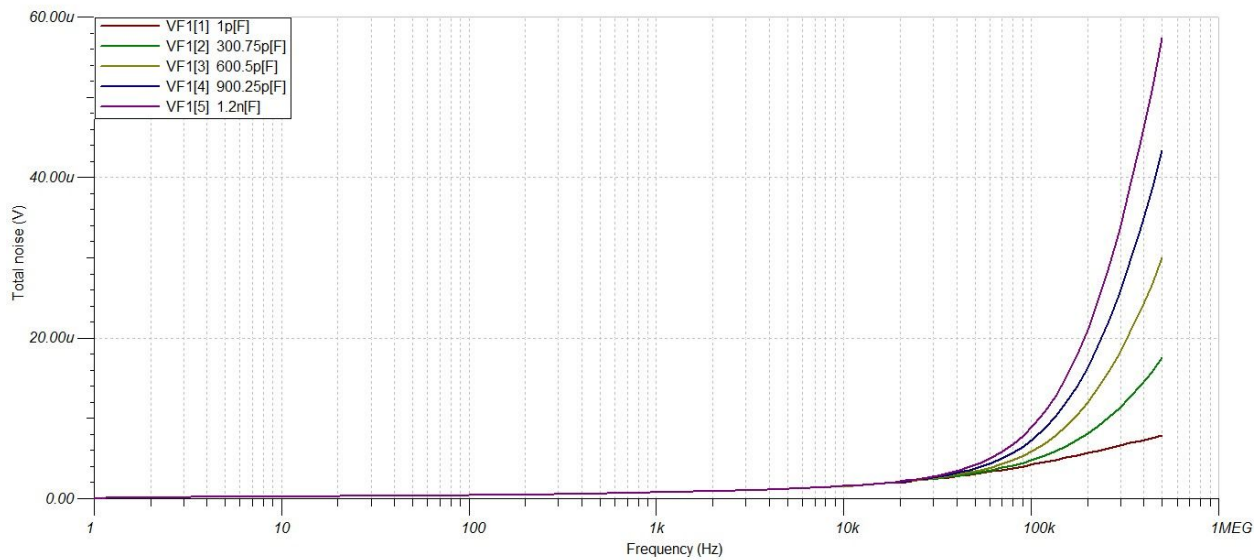
The system was simulated using TINA-TI as the SPICE simulation tool and the noise PSD, RMS and finally output SNR were determined over the frequency range of interest.



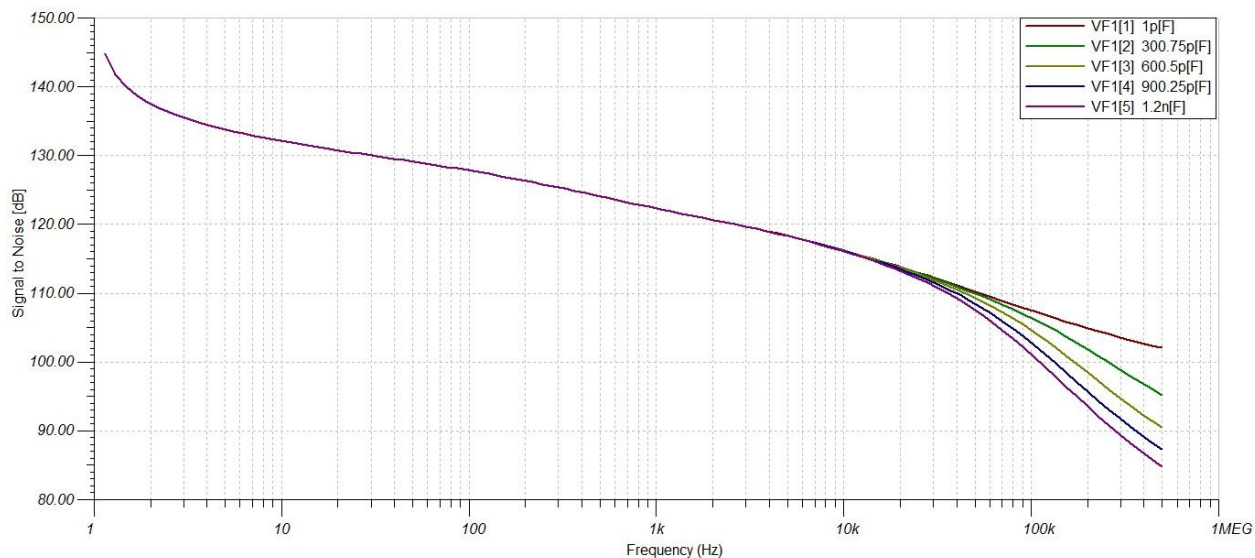
Input noise PSD



Output noise PSD



Total output noise RMS



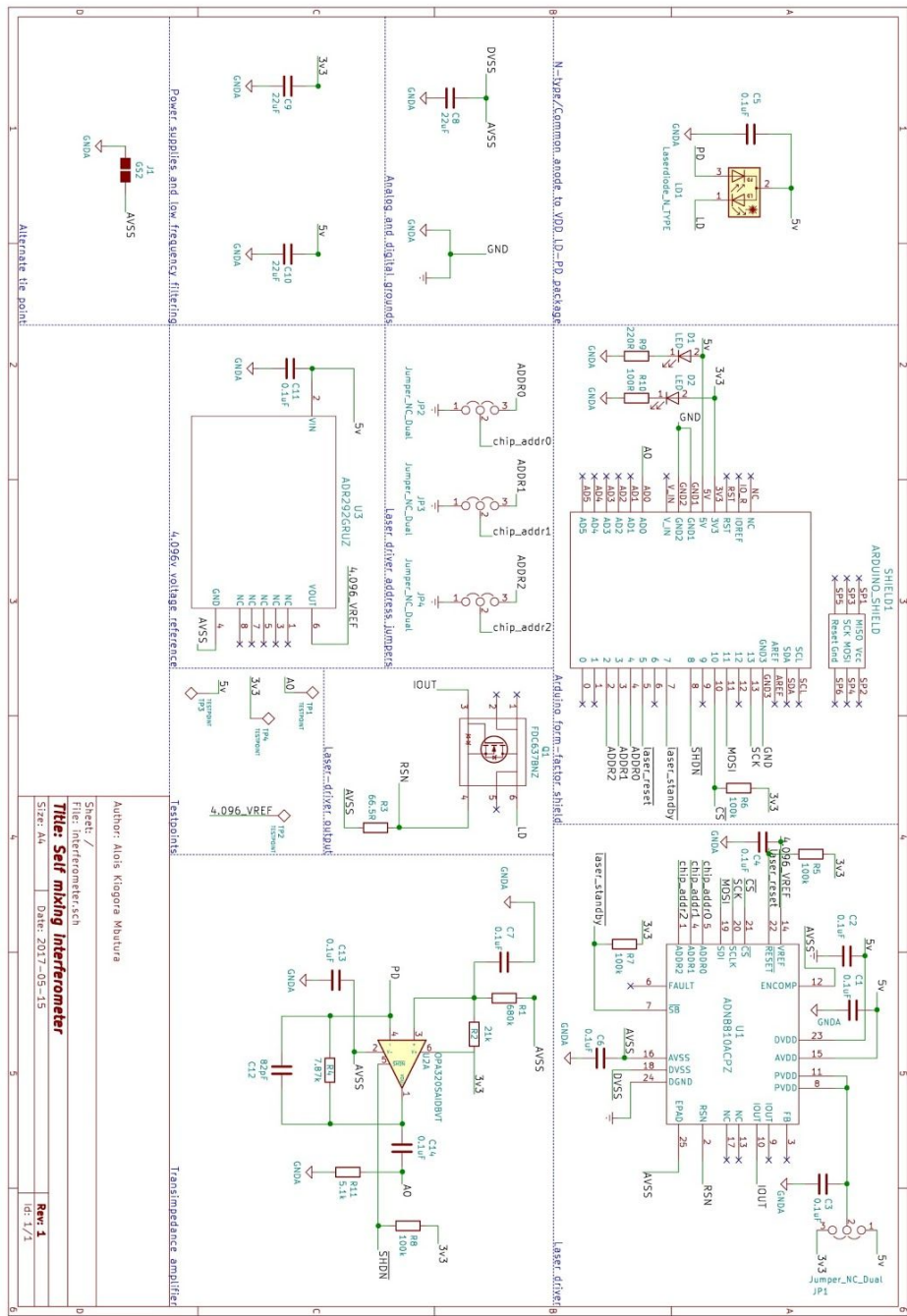
System SNR

The worst case output noise floor was determined to be 35.55uv RMS for a junction capacitance of 1.2nF at the break frequency 310 kHz. The worst case SNR for the system was determined as 89dB for the junction for the junction capacitance and break frequency value above.

Output highpass filter

The output filter is thus taken to be a high pass filter in order to prevent power supply noise and the effects of ambient light which takes the form of a constant value from the photodiode. A cut off frequency of is thus chosen and is implemented as an RC filter. The RC filter has a cutoff frequency of 312.07 Hz to present power supply noise and the effects of ambient light corrupting the output signal. R1 is chosen as 5. 1kohm and C1 is chosen as 0.1uF. The capacitor set the constraint on the resistor choice as 0.1uF capacitors are very common and it is more prudent using common capacitor values in the design unless a situation demands not to.

Schematic design



KICAD was chosen as the design program of choice due to its open and free nature. The design was made arduino form factor compatible that would liberalise the choice of the control microcontroller due to the pervasiveness of the arduino form factor in industry.

Layout design

For this design, high frequency layout design techniques were followed which include:

- Separation of analog and digital grounds.
 - Separation of power supplies.
 - Removal of copper layer otherwise known as a keepout zone around the TIA.
 - Traces crossing a plane split an any layer should do so perpendicularly to the plane split.
 - Forming a star grounding scheme whereby all grounds are tied together at the supply.
 - Having high frequency decoupling capacitors as close to the IC's as possible.
 - Tie the analog ground and the digital grounds together at the supply through a bulk decoupling 22uF capacitors.
 - Routing the amplified photodiode signal over the Analog ground plane only.
 - Elimination of stubs on any signal traces. All test points ate therefore parts of the trace that have the soldermask layer peeled back.
 - Routing over a 4 layer PCB board. With the ground plane being as close to the main signal layer.
 - Minimisation of capacitance around the TIA by having components as close as possible and on one layer without any vias.
 - Keeping all vias away from the TIA section.

The complication of this design is that a ground connection has two purposes:

- A return path for current..
 - A reference upon which voltage measurements are made. This is really important in precision circuits.

As opposed to common thinking, not all grounds have the same potential 0v. This leads to ground loops and voltage differences in the grounding scheme. The problem is made worse by voltage spikes in current spikes in the ground line. For the purposes of a good reference, the grounding scheme is recommended as a plane in order to form a low impedance path for current. The general equation for impedance is given as:

$$Z = R + j\omega L - j \frac{1}{\omega C} \dots \dots \dots (xv)$$

At DC, the current follows the path of least resistance as $\omega=2\pi f=0$ as $f=0$. The circuit in this case thus flows in order to minimise the resistance

At higher frequencies, the current follows the path of least impedance at which the $j\omega L$ term dominates while the R and $j \frac{1}{\omega C}$ diminish. Therefore the circuit flows so as to minimise the inductance. The inductance is held in the magnetic field between the supply and return currents. Therefore in order to minimise this, high frequency currents try to flow right under the supply path. Any difficulties in doing so leads to voltage spikes so as to create enough potential to

overcome the obstruction. It is a must that such voltage spikes do not affect the use of the ground as a reference this it is important to separate them.

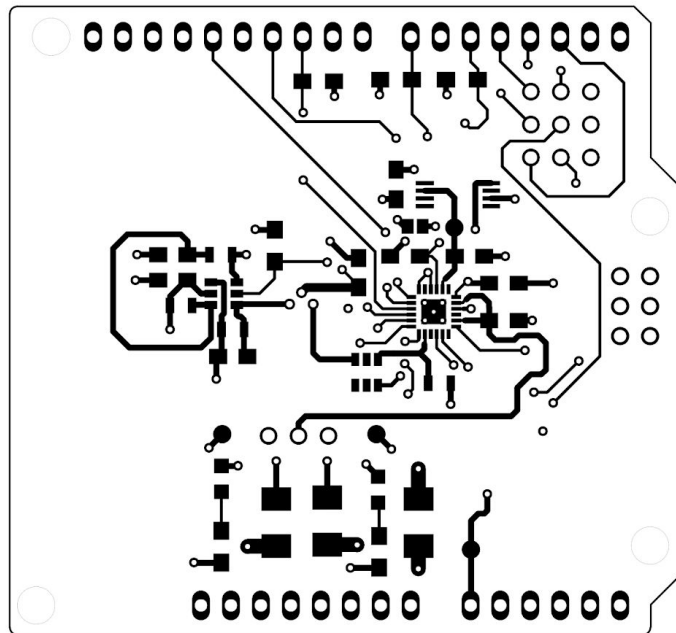
For digital circuits the main function of ground thus is:

- A return path for current.

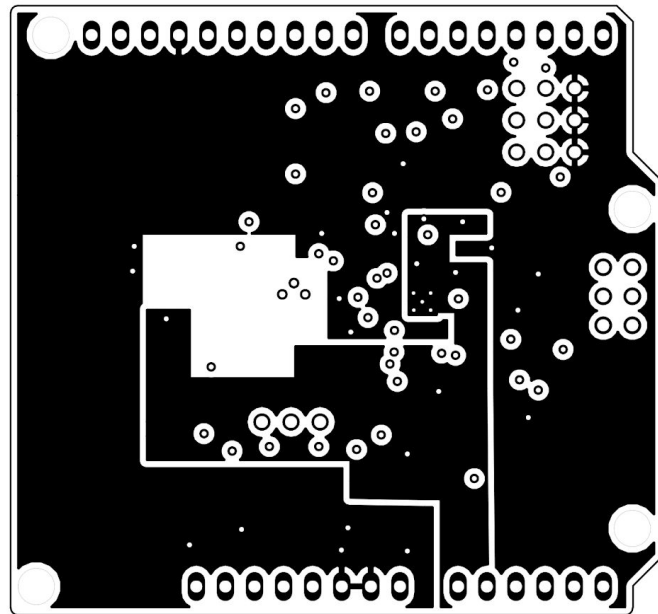
For analog circuits/precision circuits, the uses of ground are:

- A return path for current..
- A reference upon which voltage measurements are made. This is really important in precision circuits.

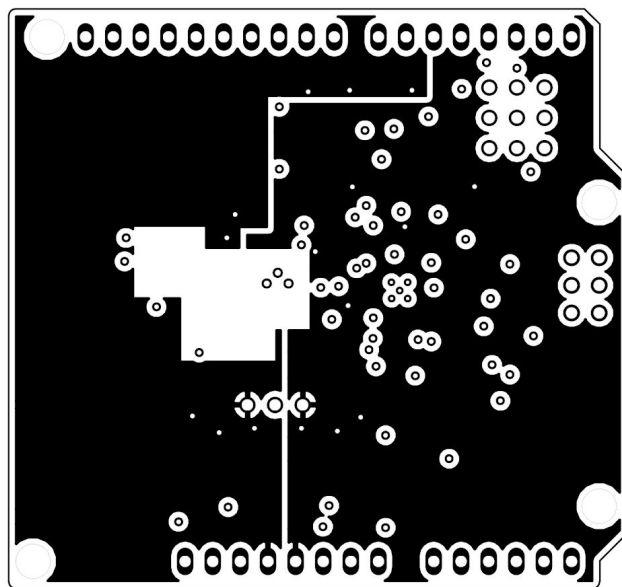
Main layout images



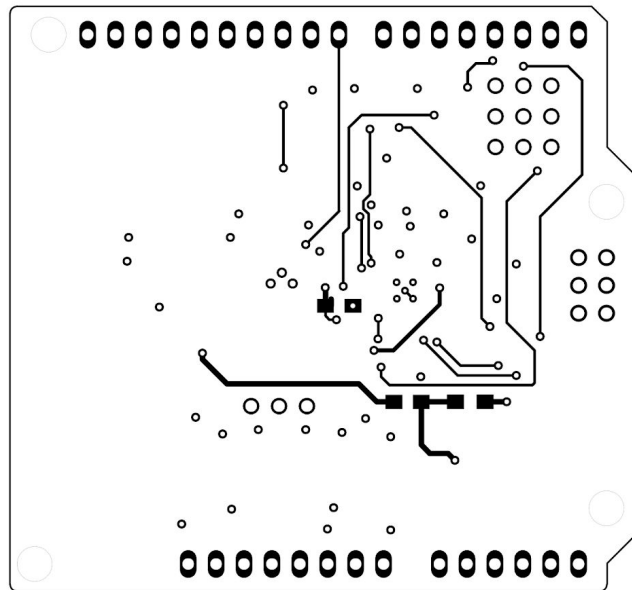
Layer 1: Top/main copper layer



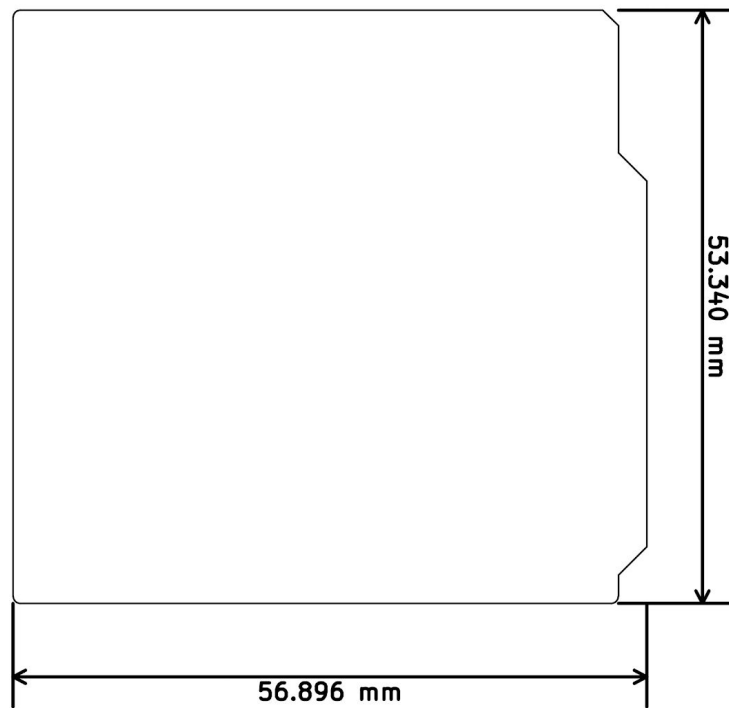
Layer 2: Analog ground/Digital ground



Layer 3: 3v3 supply and 5v supply.

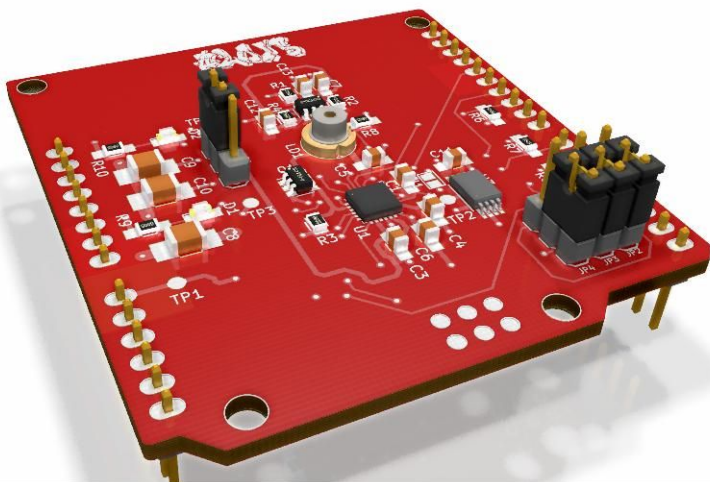


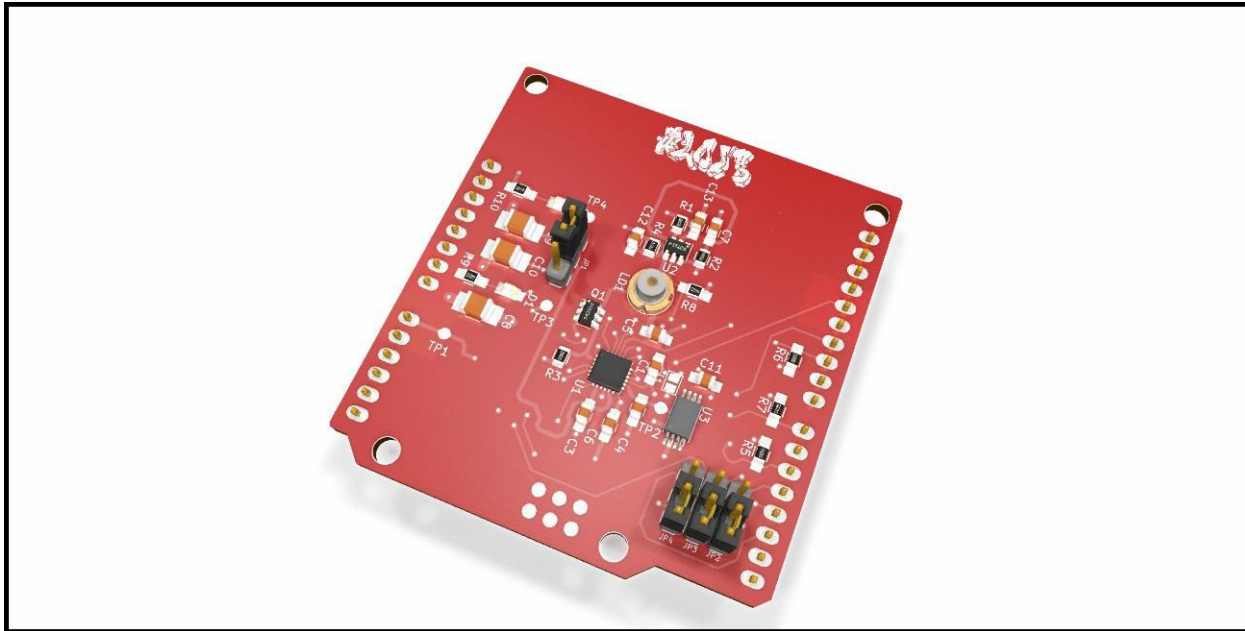
Layer 4: Bottom copper layer



Auxiliary layer: Board edge and dimensions

3D rendered, layout view





Bill of materials

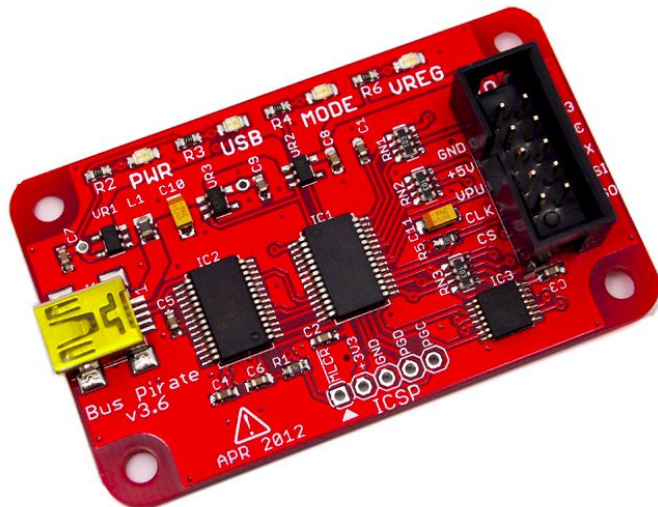
LD1	Laserdiode_N_TYPE	ADN8810ACPZ:ADL-65055TL	1
D1,D2	LED	LEDs:LED_0805	2
C8-C10	22uF	Capacitors_SMD:C_1210_HandSoldering	3
R4	7.87k	Resistors_SMD:R_0805	1
R5-R8	100k	Resistors_SMD:R_0805_HandSoldering	4
C12	82pF	Capacitors_SMD:C_0805_HandSoldering	1
R9	220R	Resistors_SMD:R_0805_HandSoldering	1
U1	ADN8810ACPZ	ADN8810ACPZ:ADN8810ACPZ	1
U2	OPA320SAIDBV7	TO_SOT_Packages_SMD:SOT-23-6	1
R1	680k	Resistors_SMD:R_0805	1
U3	ADR292GRUZ	ADN8810ACPZ:ADR292GRUZ	1
R3	66.5R	Resistors_SMD:R_0805	1
R2	21k	Resistors_SMD:R_0805	1
Q1	FDC637BNZ	TO_SOT_Packages_SMD:SOT-23-6	1
JP1-JP5	Jumper_NC_Dual	freetronics_footprints:1X03	5
SHIELD1	ARDUINO_SHIELD	freetronics_footprints:ARDUINO_SHIELD	1
C1-C7,C11>0.1uF		Capacitors_SMD:C_0805_HandSoldering	8
TP1-TP4	TESTPOINT	Measurement Points:Measurement_Point_Round-SMD-Pad_Big	4
R10	100R	Resistors_SMD:R_0805_HandSoldering	1

Fabrication

Emulating the laser driver SPI protocol

Due to the importance of the code in determining the LASER driver output current, the sending of an inappropriate codeword may overdrive the SL leading to its destruction. On thus to ensure the bit order is not reversed during transmission.

For quick testing of the SPI protocol, a device known as the bus pirate was used. The device enables sending data via various embedded protocols through a serial connection to the bus pirate from a computer.

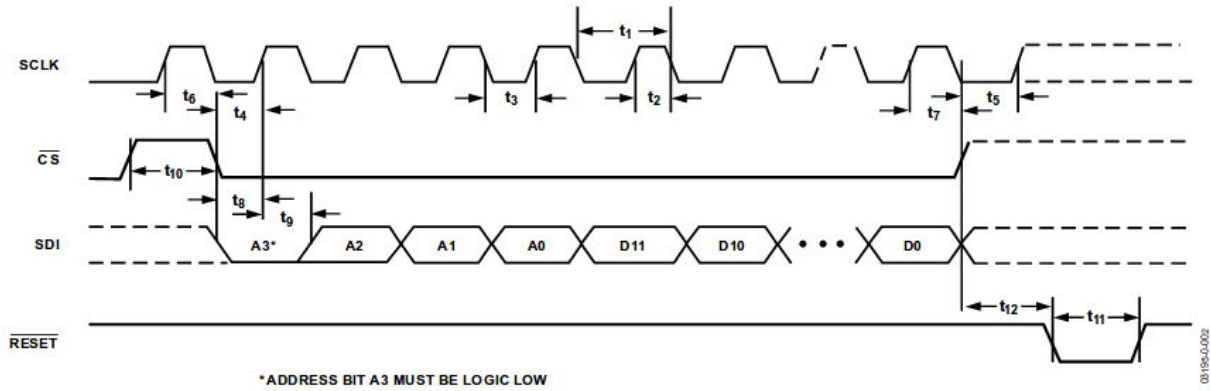


The Bus pirate



The logic analyzer used: DSlogic pro

The laser driver protocol below was emulated with the bus pirate as the master device as the communication was sent to a logic analyzer for packet sniffing and decoding:



The first bit is A3 shifted into the laser driver serial register

In our test scenario, the 12 bit laser driver data code was 0xFFFF-decimal 4095 while since we have only one laser driver in our application, we choose its' address as 0x0. The eventual 16 bit code is thus 0x0FFF. We should shift in no more than 16 bits in order to prevent the ADN8810 laser driver from shifting the leading bits out as multiple laser drivers are meant to have their data line serially connected if in use in an application.

The data register for the laser driver is 16 bits wide while for most controllers are 8 bit wide. Therefore due to this register mismatch of the sender and receiver, the CS(chip select) line of the SPI bus is used as a latch and enable signal. Therefore one should only latch the data after 16 bits are sent,

The following setup is setup between the bus pirate and the logic analyzer.

The bus pirate appears as a serial device to a computer. The following command is sent from an Ubuntu 16.04 terminal to the bus pirate after successful connection with a baudrate of 115200 and setting up the SPI mode of the device:

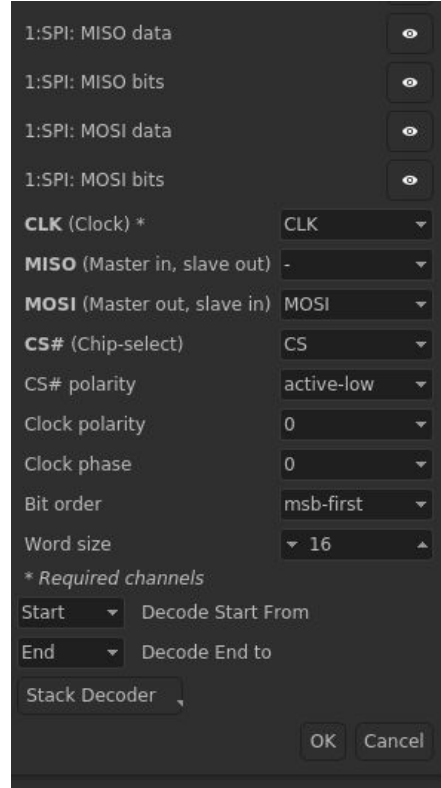
```
SPI>[0b00001111 0b11111111]
/CS ENABLED
WRITE: 0x0F
WRITE: 0xFF
/CS DISABLED
```

The “[“ character means CS line enable while “]” means CS line disable.

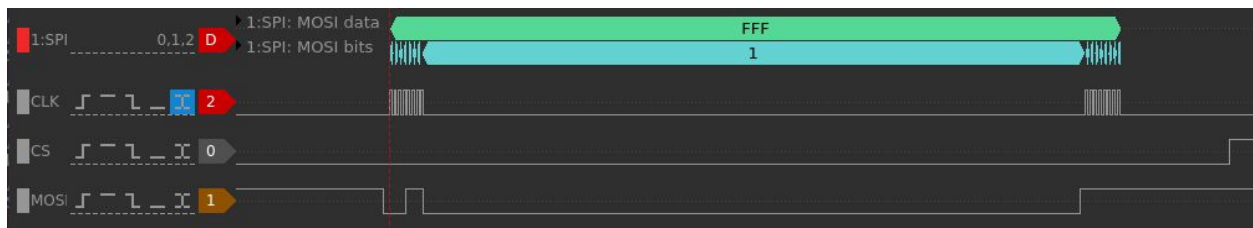
The SPI protocol is a big endian default protocol as it sends out the MSB first. This means that the bytes are arranged in 0b 00001111 11111111 from a data level point of view but the SPI hardware sends it out as 0b 1111000 11111111 on a per byte basis from a hardware/physical layer point of view but since the receiver and sender perform dual operations to each other, the data view is unchanged. This means that both sender and receiver must agree whether they are sending MSB first

per byte or LSB first for proper decoding. This is predetermined by the system designer as such information is not sent within the protocol. The receiving device determines the format. For the laser driver according to the timing diagram, this will be a little endian format.

We then set up our logic analyzer as below:



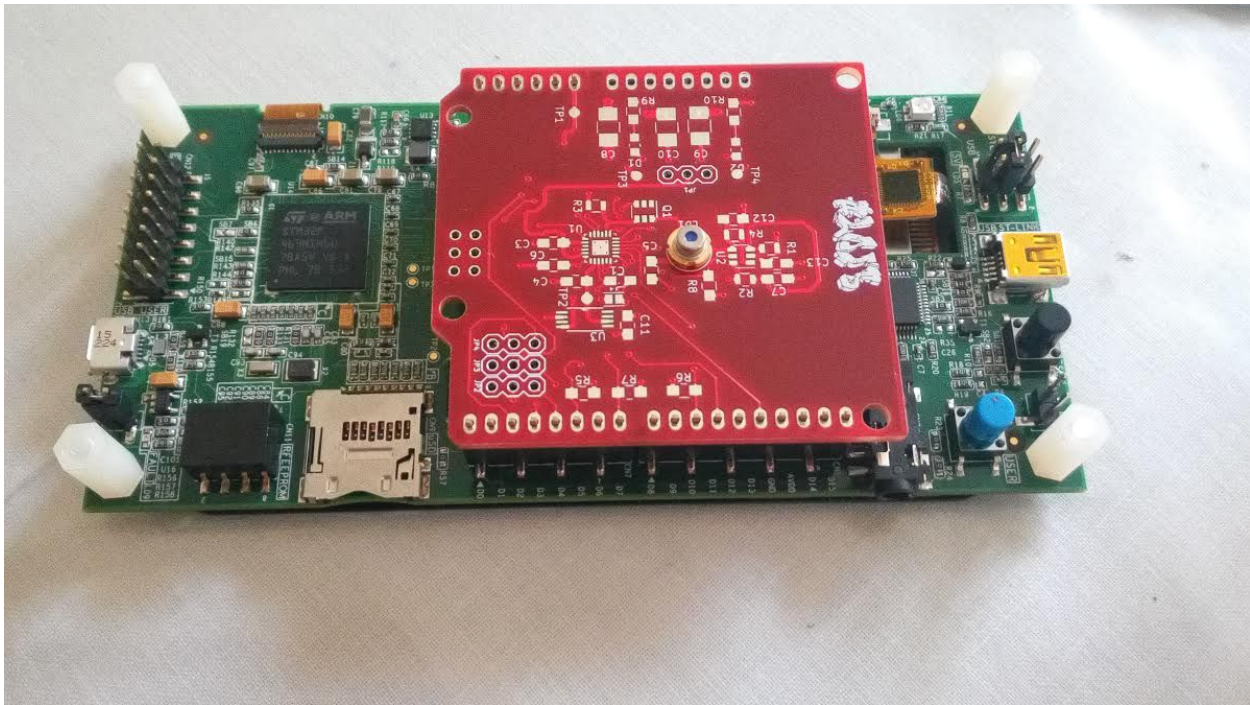
From the above we obtain the below results from the logic analyzer:



The decoded data is successfully confirmed as 0x0FFF, the same as that was sent. Time starts from left.

Pre-fabrication fitting

The 4 layer PCB was finally completed and a pre-fabrication fitting was performed with an ARM STM32 discovery board that was in reach to ensure the drill diameters were suitable especially for the SL and the arduino compatible headers as in the images below:



The pre-fabrication fitting test was successful.